MASS SPECTROMETRIC STUDIES AND CRYOGENIC REACTIVITY OF CF_2 AND Cl_2

A THESIS

Presented to

The Faculty of the Graduate Division

by

William Joseph Martin

In Partial Fulfillment

of the Requirements for the Degree

Doctor of Philosophy in the School of Chemical Engineering

Georgia Institute of Technology

March, 1965

MASS SPECTROMETRIC STUDIES AND CRYOGENIC REACTIVITY OF CF_2 AND CI_2

A THESIS

Presented to

The Faculty of the Graduate Division

by

William Joseph Martin

In Partial Fulfillment

of the Requirements for the Degree

Doctor of Philosophy in the School of Chemical Engineering

Georgia Institute of Technology

March, 1965

ACKNOWLEDGMENTS

I am deeply indebted to Dr. H. A. McGee, Jr. for the suggestion of this problem and for his interest and help, not only concerning this work, but at every stage of my graduate studies. My appreciation is also expressed to my fellow graduate students, D. B. Bivens, T. J. Malone and J. H. Wilson, for their willing assistance with many problems and to Dr. W. H. Eberhardt and Dr. W. M. Newton for their interest and their suggestions while serving as the reading committee.

The National Science Foundation, through Cooperative Graduate Fellowships in 1962-63 and 1963-64, made it possible for me to devote full time to academic work and my deepest appreciation is due for this assistance. I also wish to thank the National Aeronautics and Space Administration for their support through NASA grant NsG-123-61 administered by the Engineering Experiment Station. Several of the gases studied in this work were generously furnished by E. I. DuPont De Nemours Company, Incorporated.

The encouragement and assistance of my wife, Betti, my parents, Mr. and Mrs. J. R. Martin, and many other relatives, particularly Mr. and Mrs. D. J. Pinion, are gratefully acknowledged. The excellent typing of Mrs. Jean Smith is deeply appreciated.

TABLE OF CONTENTS

LIST OF TABLES

LIST OF FIGURES.

LIST OF FIGURES (Continued)

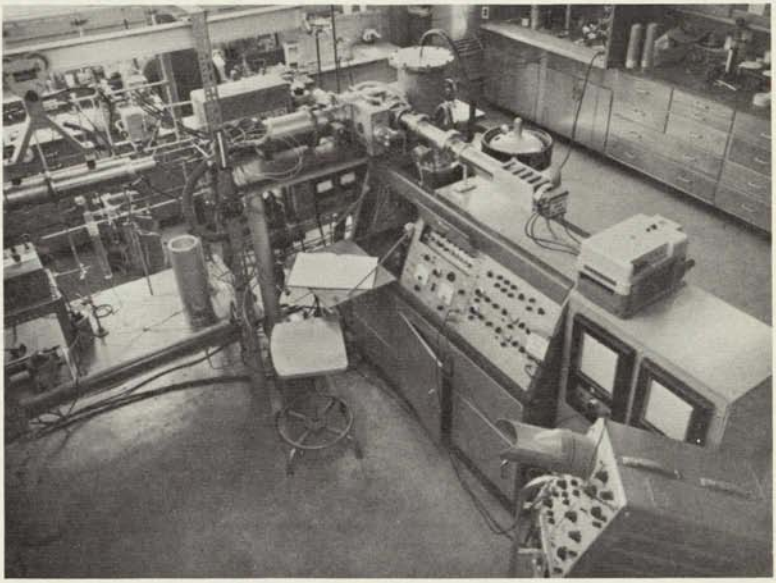

Figure 1. General View of Mass Spectrometer and Associated Cryogenic Equipment.

SUMMARY

The work reported in this thesis involved the generation of CF_2 by pyrolysis of various parent compounds, the identification and study of this molecule by mass spectrometric techniques, and the study of the reactivity of CF_2 at cryogenic temperatures. Similar experiments with CI_2 were attempted but none of the several combinations of parent compound and pyrolysis conditions yielded any evidence for the presence of free CI_2.

There has recently been considerable interest in the formation and stability of CF_2 and of the various other halogen substituted methylenes; the late 1964 dates in the bibliography of this thesis attest that this interest is current. The halogen substituted methylenes appear to be present as intermediates in a number of reactions and, in particular, several studies have indicated that CF_2 is produced in the photolysis, pyrolysis or electrical discharge of fluorocarbon vapors. Several investigations of the absorption spectrum of CF_2, either in the gas phase[4,5] or trapped in an inert matrix at 4.2° K,[6,7] have supported the conclusion that CF_2 has a singlet ground state (i.e., it is not a free radical). The half-life of CF_2, as formed in one of these experiments, was estimated to be of the order of one second.[11] An extraordinary chemical stability of CF_2 has been postulated to explain the results of experiments in which the products of a radio-frequency discharge through cyclo-C_4F_8 or C_2F_6 were deposited on a liquid nitrogen

filament. Similar studies of C_2I_4 and CHI_3 did not result in the formation of detectable amounts of CI_2.

When CF_3I was admitted to the mass spectrometer at room temperature, $AP(CF_2^+)$ was found to be 17.2 $\pm$ 0.1 ev. $AP(CF_2^+)$ was much lower, however, after passage of the parent compound over a platinum filament at 900°-1300° C and, in fact, CF_2 was present in such quantity that its vertical ionization potential could easily be determined and was found to be $I_{vert}(CF_2)$ = 11.8 $\pm$ 0.1 ev. The uncertainty attached to this number applies only to I_{vert} since the actual ionization energy is not necessarily observed in electron impact experiments. $I_{vert}(CF_2)$ obtained in the present work is considerably lower than the previously published value of 13.3 ev, but is in excellent agreement with the value of 11.7 ev reported by Fisher, Homer and Lossing.[49]

No one has previously detected CF_2 in the decomposition of CF_3I, but several studies have demonstrated that CF_3 can be produced from CF_3I by a variety of methods. In the present work, however, the method of appearance potential lowering did not indicate that free CF_3 was present in the pyrolysis gases. $AP(CF_3^+)$ from CF_3I was found to be 11.1 $\pm$ 0.2 ev and since $I_{vert}(CF_3)$ has been reported to be 10.2 ev,[56] any appreciable concentration of CF_3 would have been detected. The presence of considerable concentrations of C_2F_6 and I_2 in these pyrolysis gases would seem to indicate that CF_3 was formed at some point during this process, however.

Values of I_{vert} and AP for many other species were obtained during the course of this investigation and are given in Table 3. The mass spectra of some of the parent compounds are available in a standard

cooled surface; a blue color, claimed to be due to CF_2 persisted up to 95° K.[28]

In contrast to the wealth of information concerning CF_2, a literature search revealed no case in which CI_2 had been produced in the gas phase; the only pertinent information seems to be the formation of CI_2 in the basic hydrolysis of CHI_3.[13]

A Bendix Time-of-Flight Mass Spectrometer, with minor modifications to permit the determination of appearance potentials (AP) by the retarding potential difference (RPD) method, was used in this work. AP lowering is thought to be the most reliable mass spectrometric method for the detection and identification of unstable species in a gaseous mixture.

The decomposition of the parent species was accomplished by pyrolysis in a tubular equilibrium furnace at temperatures up to 500° C or on heated metal filaments at temperatures as high as 2000° C. In either case, care was taken to insure that the gaseous samples passed from the high temperature environment directly into the mass spectrometer ion source without recombination or further reaction; this was accomplished by the use of low pressures, close spacing and differential pumping.

CF_3I, $CHClF_2$, CF_2CFCl, cyclo-C_4F_8 and $CF_2ClCOOH$ were pyrolyzed in the search for free CF_2; the decomposition of CF_2CFCl and cyclo-C_4F_8 on heated metallic filaments resulted in some evidence for the production of CF_2 but the highest concentration of CF_2 which was found in this work was produced by the passage of CF_3I over an incandescent platinum

compilation of such data[44] but these spectra were obtained on magnetic deflection instruments. Since such spectra are not normally identical with the spectra obtained on a time-of-flight machine, the complete low resolution mass spectrum of each of the parent compounds is presented in Appendix B.

Low temperature quenching experiments were conducted in which the products of the CF_3I pyrolysis were immediately cooled to 77° K or to 4.2° K. Argon was used as a carrier gas and as an inert matrix in the experiments in which liquid helium was used as a coolant. A cryogenic inlet system allowed the effluent gases, which resulted from the warmup of these deposits, to be admitted to the mass spectrometer ion source without exposure to a warmer environment. CF_4, C_2F_4, and C_2F_6 were identified in the gases evolved during warmup of these quenched products but no free CF_2 or CF_3 was detected. The absence of a parent peak in the mass spectrum of CF_4 led to the initial hypothesis that CF_3 free radicals had been trapped and revaporized without reaction or recombination. Measurement of the appearance potentials of CF_3^+ and CF_2^+ from this low temperature gas, however, showed that this spectrum was that of CF_4. Since it has been shown that CF_2 is indeed trapped in an inert matrix at 4.2° K and convincing arguments have been presented for the stabilization of both CF_2 and CF_3 in a matrix of the parent, cyclo-C_4F_8, at 77° K, it is very likely that CF_2 and CF_3 are present in the low temperature deposits produced in this work. It must be concluded, therefore, that these species achieve sufficient mobility in the matrices to permit reaction or recombination at temperatures which do not allow sublimation

of the free species. The activation energy for the chemical loss mechanism must be extremely small.

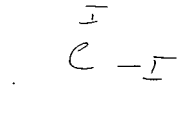

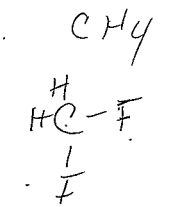

CHAPTER I

INTRODUCTION TO THE PROBLEM

Purpose of the Study

In this thesis are reported the results of one of a series of studies in the broad area of low temperature chemistry. These studies, several of which are now under way, have as their primary aims the development of preparative techniques which produce new and useful compounds, and the study of the physical and chemical behavior of these new compounds. Such studies, of necessity, also result in the design of new equipment for use at these extremes of environment and yield basic information in the field of chemical physics.

The purposes of the present work have been the generation of CF_2 and CI_2 from suitable parent compounds by pyrolysis, the identification and study of these molecules by mass spectrometry, and the study of the reactivity of CF_2 and CI_2 at cryogenic temperatures. These two compounds, at opposite ends of the spectrum of the dihalomethylenes,* were chosen for study since it seemed that they were the most likely to be stabilized at cryogenic temperatures; CF_2 because of its well-known stability in the gas phase and CI_2 because it seemed that the very large iodine atoms might provide some steric hinderance to reaction. This study was supported in part by the National Aeronautics and Space Administration

---

* Some writers refer to these species as carbenes, but this thesis will use the term "methylenes," following Chemical Abstracts usage.

through their Grant NsG-123-61 which was concerned with the preparation of highly endothermic compounds at cryogenic temperatures for possible use as rocket propellants.

During the progress of the work emphasis increasingly shifted to the mass spectrometric studies and to the measurement of ionization potentials and appearance potentials of many species. Of much interest was the measurement of the important, and previously unknown, ionization potential of CF_2. Some of the above objectives were achieved with complete success while other experiments led to negative or inconclusive results.

Dihalomethylenes

There has recently been considerable interest in the formation and stability of CF_2, CI_2 and the various other substituted methylenes. The existence of these species as reaction intermediates had been postulated as early as the middle of the 19th Century and, in several instances, these proposals have been verified by modern techniques. A review of the progress in this field, including publications through July, 1962, has been given by Hine.[1] Much of the literature concerning methylenes and methylene derivatives has dealt with mechanisms of liquid phase organic reactions, but the present discussion will be limited to that work which has to do with the production of the free species in the gas phase or with the low temperature stabilization of these molecules.

Indirect evidence for the free existence of CH_2, the parent member of the methylene series, has been accumulated for a number of years; among the most interesting of the many studies which added to this

indirect evidence was that of Rice and Glasebrook[2] who used the classical Paneth mirror technique. Only very recently, however, has there been a direct observation of CH_2 as a free entity; Herzberg and Shoosmith[3] in 1959 published a study of the absorption spectrum of CH_2 produced by the decomposition of CH_2N_2. From their results, these workers estimated the lifetime of CH_2 to be approximately 15 microseconds.

The emission spectrum of CF_2, produced by an electrical discharge through fluorocarbon vapor, was recorded and partially analyzed by Venkateswarlu.[4] In a later study of the absorption spectrum by Mann and Thrush[5] the vibrational assignments were somewhat revised. The flash photolysis of CF_2Br_2 produced the CF_2 molecules for this study. The absorption spectrum of CF_2 trapped in an argon matrix at liquid helium temperature was reported by Bass and Mann[6] and the results supported the vibrational assignments of Mann and Thrush. In this experiment CF_2 was generated in a microwave discharge through a mixture of cyclo-C_4F_8 and argon. The most recent study of the absorption spectrum of CF_2 was published in September, 1964 by Milligan, Mann, Jacox and Mitsch.[7] These workers photolyzed difluorodiazirine, CF_2N_2, *in situ* in a matrix of solid argon at 4.2° K, and the resultant CF_2 produced such a strong spectrum that the lines due to the isotopic $C^{13}F_2$ were also assigned. The results of these several spectroscopic studies indicate that CF_2 is non-linear with a bond angle of 100°-130° (Milligan, et al.[7] have proposed 108°), and that the ground electronic state is a singlet. The ground electronic state of the linear CH_2 molecule is thought to be a triplet state.[8]

From the above information the shared and unshared electrons which satisfy the valence of the carbon atoms in CF_2 and CH_2 might be assigned as shown in Figure 2.

The linear CH_2 would be of sp type hybridization and the two unoccupied orbitals would have equivalent energies. Therefore, from Hund's rules, we would expect this molecule to be a triplet, i.e., to have two unpaired electrons. The bonding in the non-linear CF_2, on the other hand, would more closely resemble that in an sp^2 hybrid. The nonbonding orbitals would no longer be equivalent and the molecule would now assume a singlet configuration.

Simons and Yarwood[9] have attributed the remarkable stability of the CF_2 molecule to the very high electronegativity of the fluorine atoms; the shared pairs would be withdrawn from the carbon atom by the strong attraction of the fluorine atoms. Hence, the carbon atom would be left deficient in electrons and the unshared electron pair would be much more tightly bound, thereby reducing the chance of reaction. These workers[10] have found that CF_2 could easily be detected 20 milliseconds after the photolysis of $CF_2ClCOCF_2Cl$. Laird, Andrews and Barrow,[11] in their study of the absorption spectrum of CF_2 generated by an electric discharge in fluorocarbon vapors, suggested that the half life was of the order of one second, and indicated that CF_2 was removed by reaction at the walls of the containing vessel. These results are to be contrasted with the previously mentioned estimate of about 15 microseconds for the lifetime of CH_2.

Another factor which is believed to be of importance in the stabilization of CF_2 is the contribution of resonance structures.[12]

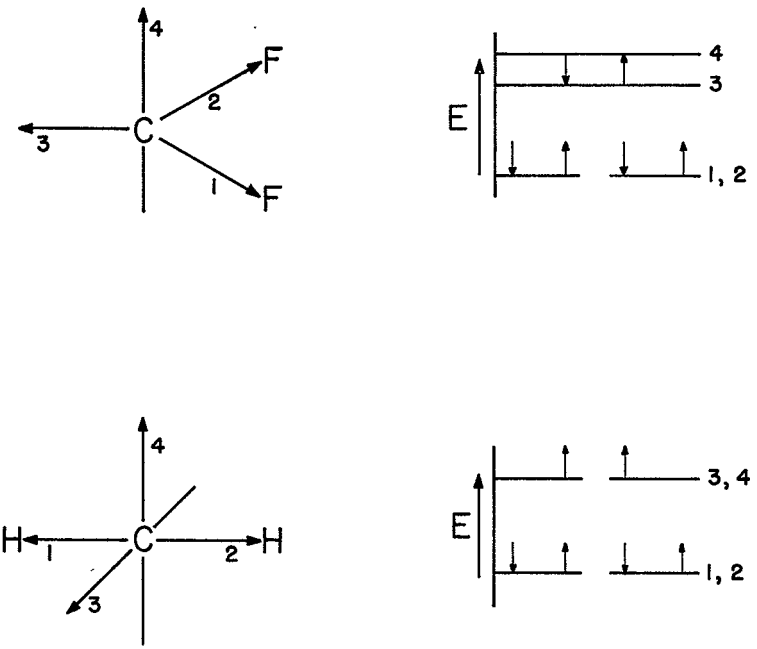

Figure 2. Possible Configurations for the Electronic Ground States of CF_2 and CH_2.

The electronic structure which is proposed in Figure 2 would require that there be non-bonding pairs of electrons on the fluorine atoms whose orbitals could overlap the empty orbital of the carbon atom (see Figure 3). Such overlapping would result in a "feedback" of electrons to the carbon atom and, hence, the structures shown in Figure 3 would contribute to the stability of the CF_2 molecule.

Very little work has been done on the CI_2 molecule and, in fact, a literature search has revealed no case in which CI_2 has been produced in the gas phase. Hine and Ehrenson[13] have shown that CI_2 is formed in the basic hydrolysis of CHI_3, but there seems to be little other evidence for the formation of this species in liquid media. These authors have pointed out that iodine stabilizes free radicals (triplets) to a much greater extent than do the other halogens but that iodine atoms lead to much less stabilization by the contribution of resonance structures such as those discussed previously for the singlet CF_2. These two effects lead to the view that CI_2 may have a triplet ground state; this hypothesis remains to be proven, however.

Generation of CF_2 and CI_2

CF_2 has been produced in the gas phase from a variety of parent compounds, some of which were mentioned above. A more complete list is given in Table 1, along with the high energy operation required for the generation of the unstable species.

Perhaps the most unusual of the methods presented in Table 1 is the pyrolysis of $(CF_3)_3PF_2$ reported by Mahler.[14] The decomposition of

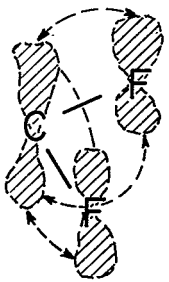

Figure 3a. Overlap of Non-Bonding Electrons of Fluorine with the Unfilled Orbital of Carbon.

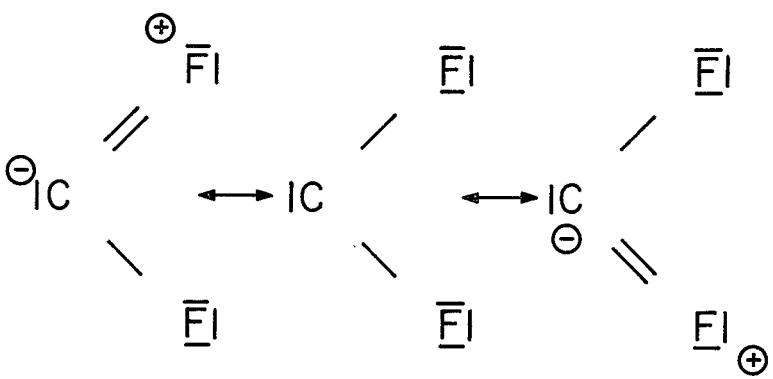

Figure 3b. Resonance Structures of CF_2.

$(CF_3)_3PF_2$ proceeds through the stepwise elision of CF_2.

$$(CF_3)_3PF_2 \rightarrow CF_2 + (CF_3)_2PF_3 \rightarrow CF_2 + CF_3PF_4 \rightarrow CF_2 + PF_5 .$$

This reaction provides gas phase CF_2 at moderate temperatures (about 200° C) and hence may prove to be a convenient source of CF_2 for studies which might be affected by the high energy environments associated with the other methods of generation of CF_2.

Mitsch[15] has recently synthesized difluorodiazirine, CF_2N_2, which has been shown to decompose at 150° to 185° C into CF_2 and N_2. A great advantage of this parent compound is the fact that the relatively inert N_2 is the only by-product.

Photolytic production of unstable species has the advantage of much lower temperature operation than is the case in discharge or thermal decomposition. In photolytic experiments the identity of the products is generally known, since use of light of the proper wave length will permit the dissociation of the weakest bond in a molecule while leaving the stronger bonds unchanged and, hence, a much less complex system is obtained.

Electrical discharge techniques have frequently been used to produce a wide variety of free radicals and unstable molecules. Dissociation is due primarily to collisions between electrons and molecules.[20] There are, of course, many modes of dissociation which may be visualized for complex molecules in a discharge, and hence there is generally little hope of obtaining a "clean" system from parent compounds which are more complex than the diatomic gases.

Table 1. Some Representative Methods for the Production of CF_2 in the Gas Phase.

Parent Compound	Energy Source	Reference
CF_4	Pyrolysis (1900° K)	16
C_4F_8	Pyrolysis	17
$(CF_3)_3PF_2$	Pyrolysis (200° C)	14
$CF_2ClCOCF_2Cl$	Photolysis	10
CF_2Br_2	Photolysis	5
C_2F_4	Photolysis	18
CF_2N_2 (difluorodiazirine)	Photolysis	7
CF_4	Electrodeless discharge	4
Fluorocarbon vapor	Electrodeless discharge	11
CF_2Cl_2	Electrodeless discharge	19
cyclo-C_4F_8	Microwave discharge	6

Pyrolysis was selected as the method of generation of the unstable species in this study. The equipment required for thermal decomposition is much simpler to construct and operate than either the photolytic or discharge techniques. Pyrolysis may also be more readily generalized to large scale production of the species of interest. Pyrolytic decomposition may result in a number of reaction products from some parent compounds, but with a number of parent species the resulting system may be expected to be relatively "clean." As discussed in Chapter II, "Apparatus and Experimental Techniques," the present work includes studies of pyrolysis in both a tubular furnace (in which thermal equilibrium was established) and on hot metal filaments.

The parent compounds which were pyrolyzed in the search for CF_2 were cyclo-C_4F_8, CF_2CFCl, $CHClF_2$, CF_3I and $CF_2ClCOOH$. CHI_3 and C_2I_4 were pyrolyzed for the production of CI_2.

Identification of the Unstable Species

As noted previously, the earliest direct identifications of the free CF_2 molecule were given by ultra-violet spectroscopy, both in emission[4] and in absorption.[11] Ultra-violet and visible spectroscopy have also provided a large proportion of the available data on other free radicals and unstable molecules. Other useful methods of detecting and identifying these species are chemical reactivity, electron spin resonance and infrared spectroscopy.

Mass spectrometry has been prominent in the study of unstable molecules since the pioneering work of Eltenton[21] and is used exclu-

mass spectrometer by a detailed mass balance if the concentrations are sufficiently high and if the electron bombardment fragmentation pattern of the parent is known. The use of low energy electrons provides a much more sensitive method for the detection of free radicals and unstable species since these species can usually be ionized by electrons of much lower energy than is required to produce the same ion from the undissociated parent compound. Mass spectrometry also allows the determination of ionization potentials and bond energies. The application of mass spectrometry to this study is discussed at length and some previous work is reviewed in Chapter II. The reasons for the choice of mass spectrometry rather than some other analytical device are also presented, and the importance of the appearance potentials and ionization potential measurements is discussed.

Cryogenic Reactivity of the Unstable Species

The study of chemical reactivity at cryogenic temperatures as it has developed may be conveniently divided into the two subdivisions of matrix isolation and low-temperature synthesis, or cryochemistry. The former, commonly called free radical trapping, involves the stabilization of free radicals by freezing in a matrix of an inert material at very low temperatures. An example of such a study is the stabilization of nitrogen atoms in a matrix of nitrogen molecules. Many of the more definitive experiments in free radical trapping were carried out under the auspices of the Free Radical Program at the National Bureau of Standards (1956-1959) and the book[22] which was published at the close of this program provides a review in depth of much of this field. A

more concise introduction to free radical trapping is contained in the monograph by Minkoff.[23] This technique has been found to result in the production of only a few tenths of one per cent of low molecular weight free radicals in the solid matrix,[24] and therefore, it must be concluded that matrix isolation methods will be of little value in any large scale preparations. For example, such small concentrations preclude the use of frozen free radicals in rocket propulsion, even though the energy release upon recombination or reaction of free radicals is usually very large.

Cryochemistry is concerned with the preparation and study of relatively pure samples of materials which may not exist at ordinary temperatures. An example of such an experiment is the preparation of O_3F_2,[25] a blood-red liquid at liquid oxygen temperature which decomposes beginning about 116° K to yield O_2F_2 and O_2. This unusual compound is prepared by an electric discharge in gaseous oxygen and fluorine, in a three-to-two ratio, contained in a vessel whose walls are cooled in a liquid oxygen bath (90° K). The properties of O_3F_2 show that cryochemical substances need not be relegated to the class of interesting but useless oddities but that this material may be of wide practical importance.* The compound is an extremely potent oxidizer and when dissolved in liquid oxygen to the limits of its solubility (about one-tenth of a mole per cent), O_3F_2 renders the oxygen hypergolic toward hydrogen and low molecular weight hydrocarbons.[26] This would allow the

---

* The Air Reduction Company has recently been awarded an Air Force contract for the production of 50 tons of liquid oxygen saturated with O_3F_2.

construction of rocket engines without ignition systems and would be of greatest advantage in propulsion systems which must be shut off and restarted during flight. The field of cryochemistry has been reviewed through 1961 by McGee and Martin.[27]

As mentioned earlier, two recent publications[6,7] have discussed the spectroscopic study of CF_2 trapped in an argon matrix at liquid helium temperature; other evidence for the low temperature stabilization of CF_2 has been obtained by Mastrangelo.[28] Since these studies and the present work provide complementary results, a discussion of these papers will be deferred to Chapter III. There have been no low temperature studies of CI_2.

The study of low temperature deposits in the present work was carried out with the mass spectrometer. The solid deposits were allowed to slowly warm up and the gases evolved were admitted to the ionization region of the mass spectrometer without contacting warm surfaces. This method of studying unstable materials depends upon the radical or unstable molecule having an appreciable vapor pressure below the temperature at which it reacts or recombines. From the above, it is clear that the method will be of more value in studies in cryochemistry than it will in free radical stabilization.

The equipment required to admit the cold samples to the mass spectrometer was designed and constructed in a related study and a complete description will soon be published.[29] The capability of this device for cryochemical analyses was demonstrated by the mass spectrometric identification of O_2F_2.[29] This provided the first direct

physical confirmation of the existence of the O_3F_2 molecule and also served to clarify its molecular structure.

The usefulness of such a low temperature analytical device is perhaps best inferred from the work of Schmeisser and Schroter,[30] who recently claimed to have prepared pure, liquid CCl_2. The effluent gases from the pyrolysis of CCl_4 in a graphite tube at 1300° C were quenched directly to liquid nitrogen temperature and yielded a yellow liquid whose C to Cl ratio and chemical reaction products were indicative of CCl_2. Further work showed that the liquid was actually an equimolar mixture of Cl_2 and C_2Cl_2,[31] but not before many confusing arguments about the claim had occurred. The low temperature inlet system, coupled with the mass spectrometer, would have provided sufficient evidence to have definitely identified the low temperature liquid.

CHAPTER II

APPARATUS AND EXPERIMENTAL TECHNIQUES

Mass Spectrometer

The major piece of equipment used in this work was the Bendix Time of Flight Mass Spectrometer, Model 12-101. This machine was chosen not only for this study, but also for use in several other closely related projects which are now under way in the Cryochemistry Laboratory. Several reasons for the choice of this particular device may be given. First, the output data are simple and easy to understand by persons not expert in specialized areas of modern physics. The converse of this is true, for example, for the nuclear magnetic resonance and electron spin resonance spectrometers. Secondly, the mass spectrometer will detect all species and not just free radicals as does the electron spin resonance spectrometer. And, thirdly, the Bendix instrument is designed such that it was relatively a simple problem to modify and adapt it for the introduction of a cryogenic sample. The absence of the magnets of a deflection type mass spectrometer makes for an open structure which is readily amenable to the assembly of complex cryogenic dewars and associated apparatus around the ion source. In addition, the very short time required to record a complete spectrum is a unique advantage; typically, this time is about 15 seconds.

The Bendix machine consists, in essence, of an ion source and an ion collector which are situated at opposite ends of a highly evacuated

drift tube. The gaseous substance to be analyzed is injected into the ion source (shown in Figure 4) and a portion of the molecules are ionized by electron impact. The ionizing electrons are generated from an incandescent filament (A) and are admitted across the ionization region by the control grid (B). The slits in the control grid and the ground potential grid (C) collimate the electrons into a well defined beam with a cross-section of 1/16 in by 5/16 in. The electron trap (D) is maintained at a positive potential (usually 150 v) to remove the electrons from the ionization region.

The ions formed by this electron beam are withdrawn in bunches from the ion source by a voltage pulse applied to the three ion grids (E). The accelerating field causes each ion to reach a velocity which is proportional to the square root of its mass to charge ratio, $\sqrt{\frac{m}{q}}$, and, therefore, the original ion bunch separates as it passes through the field free drift tube into many smaller bunches, each containing ions of a specific mass to charge ratio. As a result, the light ions reach the collector first, followed by bunches of increasingly heavier ions; a temporal separation is achieved rather than the spacial separation of a magnetic deflection mass spectrometer.

The ion bunches are detected and amplified by a magnetic electron multiplier and the output is displayed instantaneously on a Tektronic Model 543A oscilloscope. The data are also recorded on a Honeywell Visicorder, Model 906C, by means of two Bendix Model 321 Scanner units which can be set to pick up the ions arriving at any time, i.e., monitor the ion current at a certain mass, or which can be made to sweep across these arrival times and, hence, scan the entire spectrum. (A more complete description of the Bendix machine may be found in reference 20.)

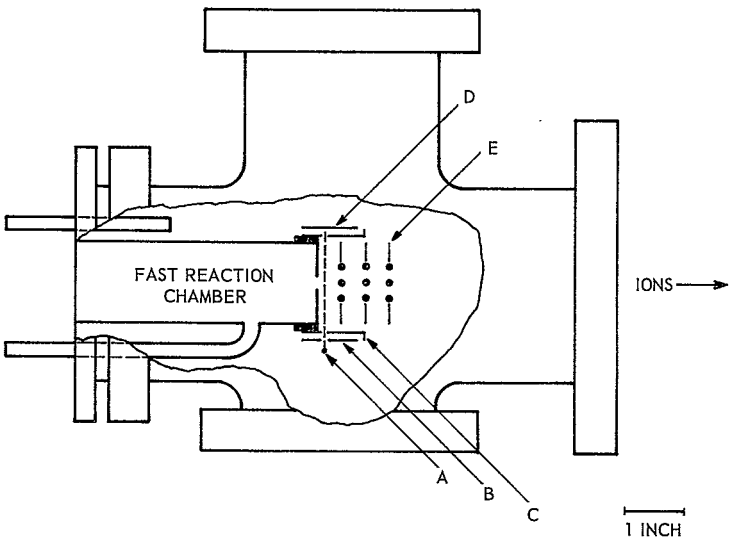

Figure 4. Mass Spectrometer Ion Source. (The electron gun has been rotated 90 degrees for clarity.)

Measurement of Appearance Potentials and Ionization Potentials

Introduction

The measurements of appearance potentials of various species are important to this work for several reasons. First, several of the ionization and appearance potentials determined during the course of this study have not been previously reported and, hence, represent a contribution to the literature of this field. Of more direct interest is the fact that appearance potential measurements allow the positive identification of unstable species in a gaseous mixture, as was first demonstrated by Eltenton.[21] This application has been briefly discussed in the introduction to this thesis. These appearance potentials can be used to compute bond dissociation energies and also, experimentally observed ionization potentials are thought to provide the most reliable basis for checking molecular orbital calculations.[33]

The procedure used for the experimental determination of the appearance potentials follows closely that presented by Melton and Hamill[34] and employs the Fox Retarding Potential Difference[35] (RPD) method. This procedure is well suited for use with the Bendix T-O-F mass spectrometer and is generally thought to be the most accurate electron impact method available without very elaborate apparatus. There has been some criticism of the RPD method, but experimental studies have shown this technique to reproduce a number of spectroscopic values within the limits of experimental error.[36]

Theoretical

The ionization potential of a molecule or an atom is defined to be the energy required to remove an electron from the neutral species in its ground state to form an ion in its ground state. For the purposes of electron impact studies this definition is not always suitable since it may be impossible to form the ion in its ground state. Hence, the electron impact ionization potential is defined to be the minimum energy of the bombarding electrons which is required to produce ionization. This, obviously, will be dependent upon the sensitivity of the apparatus. Similarly, the appearance potential of a fragment ion is defined as the minimum energy of the electron beam required to produce the fragment from a particular parent compound.

While it is not the purpose of this discussion to consider in depth the theoretical aspects of ionization processes, a short account is necessary in order to understand the differences between the ionization potentials obtained by electron impact and those obtained spectroscopically.

These processes may be conveniently illustrated on a Franck-Condon diagram for a general diatomic molecule (see Figure 5). The adiabatic ionization potential of the general molecule, XY, is represented by the dotted line connecting the ground states of the neutral molecule and the molecule ion. This is the spectroscopic ionization potential, obtained from the Rydberg series, and agrees with the first definition given above.

The Franck-Condon principle states, in effect, that the electronic transition takes place in negligible time in comparison with

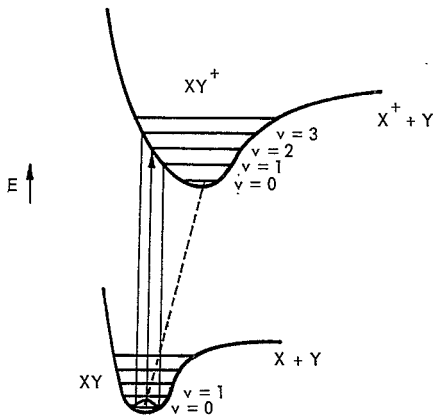

Figure 5. Franck-Condon Diagram for a General Diatomic Molecule.

that required for movements of the nuclei, i.e., the internuclear distance, r, remains constant throughout the ionization process. Obviously, then, electron impact ionization potentials will be represented by vertical lines on a Franck-Condon diagram. The most probable value of the internuclear distance for the ground state neutral molecule will lie at the center of the v=0 vibrational state on the Franck-Condon diagram and the most probable state of the molecule ion in this example will be the excited state indicated by v=3. However, there is a finite probability that the ground state neutral molecule will have an internuclear distance within the double lines and, hence, ions of lower energy may be formed in the v=2 and v=1 states. If the experiment is sensitive enough, the ionization potential determined by electron impact will be the difference in energy of the ion in the v=1 state and the ground state neutral molecule. For this particular example, the electron impact ionization potential will not agree with the adiabatic value and, in general, electron impact values can be thought of only as upper limits for the spectroscopic values.

Despite this fundamental difficulty and the fact that spectroscopic ionization potentials can be measured with a much greater degree of accuracy, electron impact values are of great importance. For many molecules, the ground state dimensions and configuration of the parent and the ion will be very nearly the same and the two methods will agree within experimental error. In a great many other cases, it is not possible to make an unambiguous assignment of the Rydberg bands and therefore an adiabatic ionization potential cannot be obtained. Except for a few cases in which the molecular ion is too unstable to be

collected, electron impact studies will always yield a value. In addition, the electron impact studies can be done in a short time and yield the ionization potentials directly. Kiser and Gallegos[37] have presented a technique which allows determination of ionization and appearance potentials in less than a minute and which is claimed to be accurate to 0.2 ev for several classes of molecules. The ionization potentials of many free radicals have been obtained by electron impact techniques since the first measurement of the ionization potential of the methyl radical by Hipple and Stevenson in 1943,[38] but only in recent years have a few free radical ionization potentials been obtained by spectroscopic methods. One prominent example is the measurement of the ionization potential of CH_2 by Herzberg reported in 1961.[39]

To avoid confusion, the symbols I and I_{vert} will be used to represent the spectroscopic and vertical ionization potentials respectively throughout the remainder of this thesis. It must be remembered that I_{vert} can be regarded only as an upper limit for I, or $I_{vert} \geq I$.

For the general molecule, XY, the vertical ionization potential, I_{vert} (XY) and the appearance potential of the Y^+ ion, $AP(Y^+)$ from XY, are the energies required for the respective processes.

$$e + XY \rightarrow XY^+ + 2e \qquad (1)$$

$$e + XY \rightarrow X + Y^+ + 2e \qquad (2)$$

The appearance potential may be expressed as the sum of several energies.

$$AP(Y^+) = D(X\text{-}Y) + I(Y) + K + E \qquad (3)$$

D(X-Y) represents the dissociation energy of the X-Y bond; I(Y) is, as above, the ionization potential of Y; and K and E are the kinetic and excitation energies of all fragments. It has been shown that, in many simple cases, K and E can be neglected and it is often assumed that this is the case for more complicated molecules.[40] Other modes of dissociation can be visualized and great care must be taken to properly identify the dissociation process. For this reason, it is important to observe the negative ion spectrum in order to recognize processes such as

$$e + XY \rightarrow X^- + Y^+ + e \quad (4)$$

For this case the appearance potential will involve the electron affinity of X, EA (X), as well as the terms of Equation (3).

$$AP(X^-) = AP(Y^+) = D(X-Y) + I(Y) - EA(X) + K + E \quad (5)$$

Consider the process of Equation (2). If we disregard the kinetic and excitation energy terms we find that for the molecule XY,

$$AP(Y^+) = D(X-Y) + I(Y) . \quad (6)$$

However, if the species Y is present in the gaseous mixture injected into the ionization chamber, the appearance potential from Y would be found to be

$$AP(Y^+) = I(Y) . \quad (7)$$

From these two equations, it is apparent that the appearance potential of Y^+ from XY is greater than that from Y by the dissociation

energy of the X-Y bond, D(X-Y). This is of major importance for two reasons, first, provided that we do not encounter the pair production process of Equation (4), the presence of decomposition products in a gaseous mixture can be definitely established, whether these products are free radicals or singlets, stable or unstable, and at much lower concentrations than can be detected by the material balance method. The appearance potential of an ion from a stable parent can always be measured and a much lower appearance potential of this ion must be regarded as evidence for the presence of the corresponding neutral species. The existence of particular intermediates in gas phase reactions, e.g., at high temperatures, can be proven.

Second, bond dissociation energies can be calculated by the use of Equation (8),

$$D(X-Y) = AP(Y^+) - I(Y). \qquad (8)$$

Here, of course, an accurate value of I(Y) is desirable, but since Y is often a free radical or other unstable species, the experimental techniques may be much more difficult than those required for the measurement of $AP(Y^+)$. In most cases of interest to this work, vertical ionization potentials must be used since spectroscopic values are not available. Several procedures have been developed for introducing these labile substances into the mass spectrometer ionization region since the pioneer work of Eltenton,[21] and the procedures used in this study are described later in this Chapter. As mentioned previously, the vertical ionization potentials for many important free radicals are available in the literature.

For processes in which kinetic or excitation energies are significant, these terms may be accounted for by replacing the equalities of Equations (6) and (8) by inequalities.

$$AP(Y^+) \text{ from } XY \geq D(X\text{-}Y) + I(Y) \tag{9}$$

$$D(X\text{-}Y) \leq AP(Y^+) - I(Y) \tag{10}$$

The measurement of these kinetic or excitation energies is beyond the scope of the present work.

Experimental Methods

Reviews of the various methods that have been used for ionization and appearance potential measurements are available in several references,[41,42,43] but the attention here will be directed toward the Fox retarding potential difference method which is thought to give the most accurate results.

The measurement of ionization and appearance potentials would be relatively simple if all the electrons in the electron beam possessed the same kinetic energy. This energy would be measured by the potential difference between the filament and the ionization region. For such an idealized case, the ion current for the species of interest would be determined at a series of electron energies. A plot of ion current vs. electron energy, called an ionization efficiency curve, would intercept the energy axis at the critical potential (see Figure 6).

There are, however, three sources of uncertainty in the kinetic energy of the electron beam: (1) the distribution of initial kinetic energies of the thermally-produced electrons (see Figure 7); (2) the

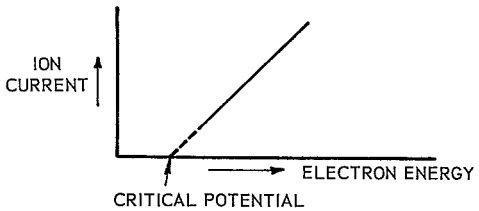

Figure 6. Idealized Ionization Efficiency Curve.

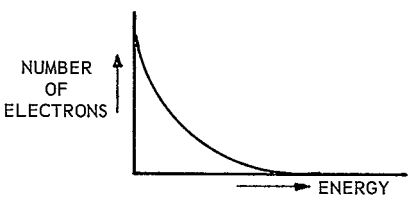

Figure 7. Kinetic Energy Distribution of Thermally-Produced Electrons.

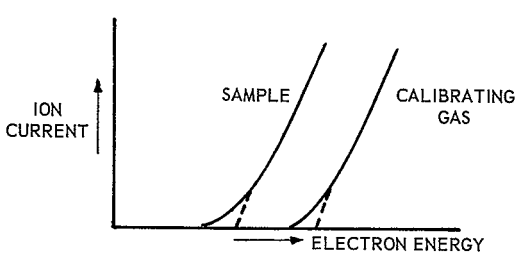

Figure 8. Ionization Efficiency Curves Illustrating Use of Linear Extrapolation Method.

unknown contact potentials, i.e., any voltage drops which make the electron energy different from the bias measured between the filament and ground; (3) the acceleration of the electrons by the potential of the electron trap. The third effect is often neglected, but it can be greatly decreased by lowering the trap potential. The trap also is shielded to prevent ions formed in the neighborhood of the trap from drifting into the ionization region. The second of these three effects is usually accounted for by the use of a calibrating gas, often a rare gas. The contact potentials and other systematic errors will be constant, regardless of the gas under study, and hence, we can group these into one correction term whose magnitude is determined by the measured difference between the sought for ionization potential and the known potential of the calibrating gas.

There remains the problem of distribution of initial kinetic energy. This spread of kinetic energies is such that when the potential difference between the filament and the ionization region is reduced below the critical potential there will remain some electrons with sufficient energy to produce ionization. The ionization efficiency curve will now approach the energy axis in an exponential manner since thermal electrons have an exponential energy distribution (see Figure 8) and it becomes very difficult to determine a point of onset of ionization. This depends upon both the operator and the instrument sensitivity, and hence the "vanishing current" technique is seldom employed. A more common method involves extrapolation of the linear portion of the ionization efficiency curve to the energy axis (see the dotted portion of Figure 8). This "extrapolated linear intercept method" has had consid-

erable success when the ionization efficiency curves of the sample gas and the calibrating gas were of similar shape. These curves cannot always be expected to have similar shapes, however, since it has been shown that for several molecules, the ionization cross section varies significantly with electron energy.[48] The technique, of course, fails for molecules which yield ions that have excited states very near the ionization potential.

The study of the effect of a nearly mono-energetic portion of the electron beam would be a much more satisfactory solution and this is what is accomplished by the use of the "retarding potential difference" (RPD) method. Three more grids are added to the electron gun (see Figure 9); grids 2 and 4 serve as shields for grid 3, the retarding grid. As before, the control pulse is applied to grid 1, and the grid nearest the ionization region is maintained at ground potential. A small negative potential (-0.2 to -0.6 v) is applied to the retarding grid and prevents the passage of all electrons whose initial kinetic energy is less than this value (see Figure 10). This energy cut off is very sharp.

The electron beam is now retarded by applying a further bias, Δv (-0.1 to -0.2 v), to the retarding grid (see Figure 11). The electrons which are removed from the electron beam by this retarding potential are of a very small energy spread and the change in ion current, Δi, due to this retarding potential, Δv, is the ionization caused by the electrons of this energy. When the electron energy is above the critical potential there will be a small Δi due to Δv, but if the electron energy is below the critical potential Δi should be zero.

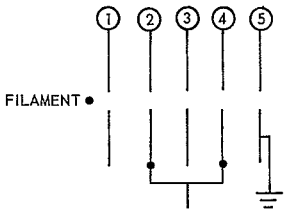

GRID	TYPICAL POTENTIAL
1. CONTROL GRID	CONTROL PULSE
2. RETARD SHIELD	FILAMENT +2.0 VOLTS
3. RETARDING GRID	FILAMENT -0.2 TO -0.4 VOLTS
4. RETARD SHIELD	FILAMENT +2.0 VOLTS
5. GROUND	

Figure 9. Electron Gun for RPD Studies.

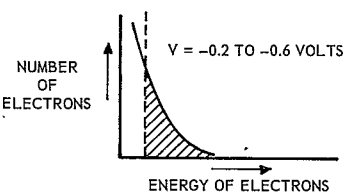

Figure 10. Effect of Application of Retarding Potential.

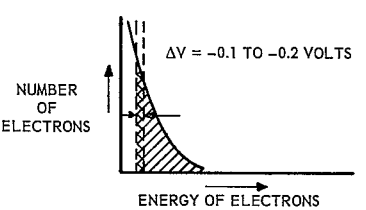

Figure 11. Effect of Retarding Potential Difference.

By recording Δi corresponding to Δv at a series of values of electron energy we can accurately locate the appearance potential. A plot of Δi vs. electron energy will intersect the energy axis at the uncorrected critical potential. The bias is returned to its original value after being retarded to insure that there has been no drift in the ion current.

As an illustration of the technique, an actual strip chart recording of an RPD study of AP(CHI_2^+) from CHI_3 is shown in Figure 12. The ionization efficiency curve derived from these raw data is also shown in this figure. Note that the voltage scale of each of these figures is uncorrected.

In order to check the accuracy of the potentials determined in this study, $I_{vert}(O_2)$ and $I_{vert}(N_2)$ were measured and, together with the previously determined spectroscopic and electron impact values, are presented in Appendix D. AP(I^+) from I_2 and AP(I^+) CF_3I, as determined in this study and as given in the literature, are also listed. These data indicate that the experimental error associated with this procedure is not more than 0.1 ev.

Apparatus

Only minor modifications on the Bendix T-O-F mass spectrometer are required for ionization and appearance potential work. The control grid pulse height was reduced from approximately 40 volts to 8 volts and the control grid bias was changed from -10 volts to 0 volts. These changes are discussed in the paper by Melton and Hamill.[34] The standard electron energy potentiometer was replaced by a Beckman Model 8221 dual

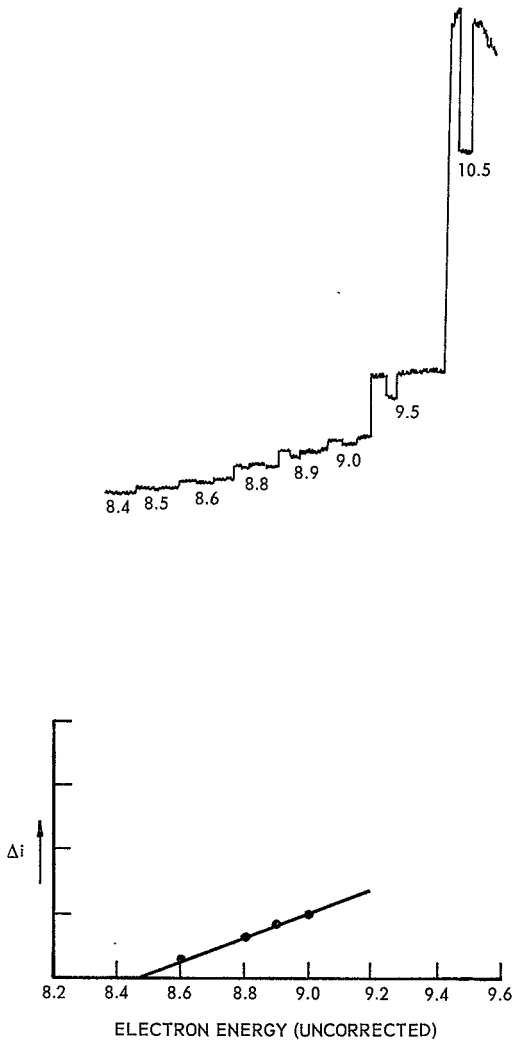

Figure 12. Sample Strip Chart Recording and Resulting Ionization Efficiency Curve for AP (CHI_2^+) from CHI_3.

ten-turn helipot as recommended by Bendix in order to obtain much closer control over the electron energy.

The potentials on the retarding grid and the retarding grid shields are maintained by means of the circuitry shown in Figure 13. This is somewhat modified from the schematic given by Melton and Hamill to allow much faster operation. The retarding potential was applied by simply throwing a switch rather than resetting a potentiometer as done by Melton and Hamill. The potential differences between the filament and ground and between the filament and the grids were measured by means of a Cimron digital voltmeter, Model 6000. The digital voltmeter provided almost instantaneous readout of the voltage applied to it and hence allowed many readings to be taken in a relatively short time. A Leeds and Northrup Model 8686 millivolt potentiometer, which was claimed by the manufacturer to have limits of error of $\pm$ 0.05 per cent, was used to check the accuracy of the digital voltmeter. No deviations were observed on the most sensitive (1 millivolt) scale of the digital voltmeter.

This same apparatus is also suitable for use in many other studies. For example, it is being used in an attempt to identify BH_3 in the pyrolysis products of B_2H_6 and, if this is successful, to measure $I_{vert}(BH_3)$.

Inlet Systems

One of the basic requirements of this study was the mass spectrometric identification of both stable compounds and unstable, highly reactive species in gaseous mixtures. This involved the introduction

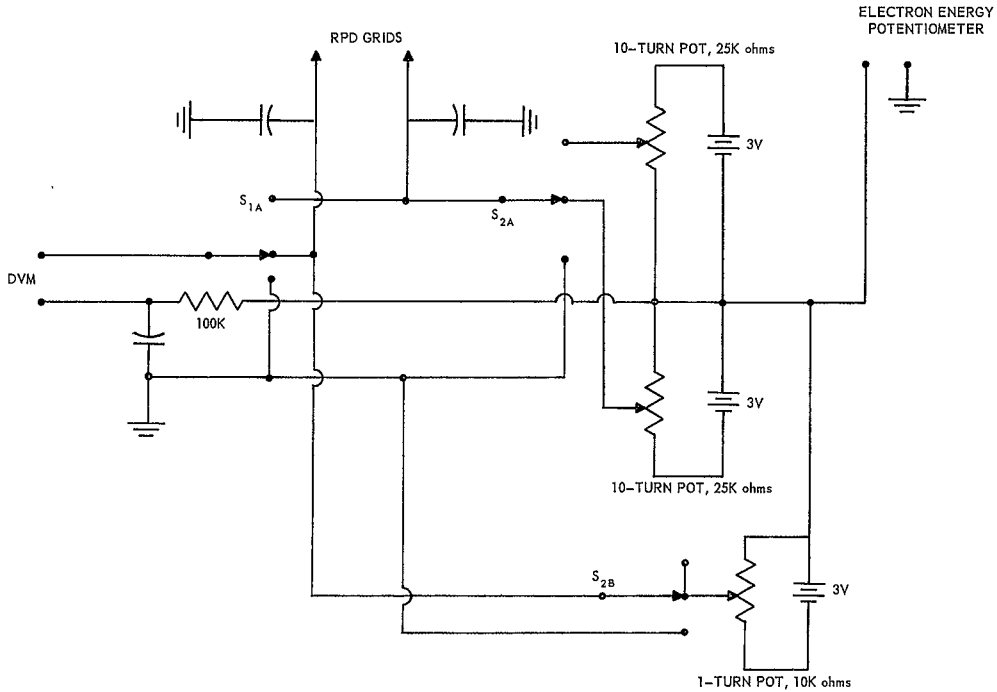

Figure 13. RPD Grid Circuitry.

into the ionization region of pyrolysis gases with no further reaction, as well as the introduction of the vapors over cryogenic condensed phases without their prior warmup. In order to insure that the gaseous samples passed from the high temperature or from the cryogenic environments into the mass spectrometer ion source without reaction or recombination, it was necessary to provide an essentially collision free path; this was accomplished by the use of low pressures, close spacing and differential pumping.

The inlet systems described below include a furnace which permitted the pyrolysis of gaseous or condensed phase parent compounds at temperatures up to about 500° C and a hot filament inlet system for use at much higher temperatures (up to 2500° C with a tungsten filament). A brief description of the cryogenic inlet system used in this work is also given.

Coaxial Furnace Inlet System

The tubular furnace shown in Figure 14 was designed for pyrolysis studies at temperatures up to 500° C and was mounted coaxially with the drift tube, inside the fast reaction chamber on the ion source header (see Figure 4).

In order to study the equilibrium vapor over C_2I_4 and other easily volatile solids as a function of temperature, it was necessary that this inlet system be capable of handling solid materials. Such a system must include a heating unit or boiler to maintain a suitable vapor pressure over the solid parent and a separate furnace to heat the vapor to the desired decomposition temperature. In addition, the gas

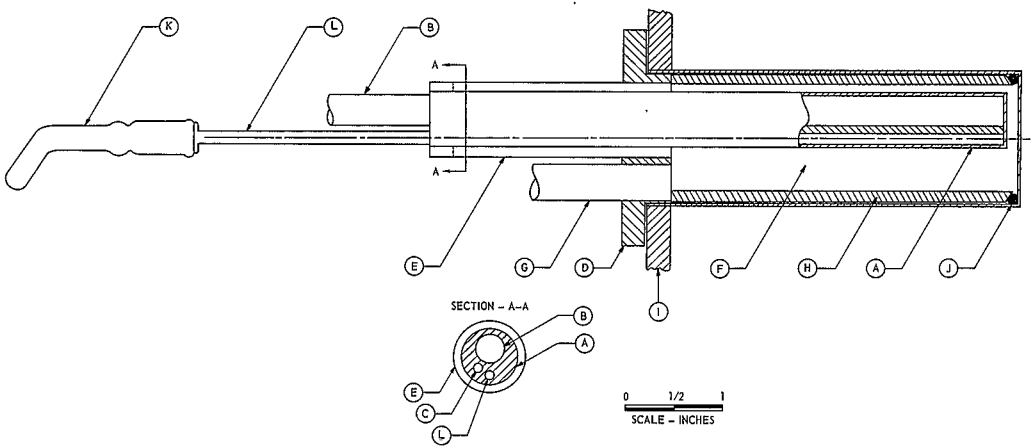

Figure 14. Schematic Diagram of Coaxial Furnace Inlet System.

handling system between the boiler and the furnace must be always at least as warm as the former to prevent the premature condensation of the vapor and consequent lowering of the pressure in the furnace.

The furnace tube itself was made of a copper rod (A) in which three holes were drilled lengthwise. One of these was lined with a monel tube and served as the heating chamber for the substance being pyrolyzed. It has a 0.030 in. diameter outlet in its bottom and the remaining two holes dead end about 1/8 in. from the outlet end of the furnace and hold an immersion heater (B) and a movable chromel-alumel thermocouple, (C), which was sheathed in a one-sixteenth inch stainless steel tube. At 100° C the furnace exhibited a temperature gradient of only 2° C over the 4 inches nearest the spectrometer.

The furnace was insulated from the header (D) by a thin-walled (0.010 in.) monel standoff tube (E). The header was designed to bolt directly to the ion source header (I) of the spectrometer with the vacuum seal made by an aluminum gasket. The fast reaction well (F) thus served as an intermediate pumping volume and was pumped out through the vacuum line (G), by a diffusion pump which was independent of the mass spectrometer pumping system.

This intermediate pumping volume was separated from the mass spectrometer by a 0.002 in. pinhole in a 0.001 in. thick gold foil. The foil was held against the end of the fast reaction chamber by a compression cylinder (H) and a Viton O-ring (J).

The sample was held in the sample tube (K) and both this tube and the delivery tube (L) connecting it to the furnace were heated by a single flexible heating tape.

The coaxial furnace was also used for investigations of the pyrolysis of gaseous compounds. For this purpose a gas handling system basically consisting of a one-liter flask and a Whitey Model 2RS4 control valve was employed. The one-liter flask provided sufficient volume to insure that the flow remained relatively constant during the time required for the experiments.

The inlet system was constructed so that the outlet of the furnace was within 1/8 in. of the electron beam of the mass spectrometer. At the pressures at which the intermediate pumping volume was operated (10^{-4} to 10^{-5} mm Hg) the mean free path of the gases was estimated to be of the order of 10 cm so that molecular flow was obtained. The residence time of the gas in the furnace was estimated to be at least 4×10^{-3} seconds which would seem to insure the attainment of thermal equilibrium. On the average, the molecules in the furnace will collide with the walls 515 times during this 4×10^{-3} sec. residence, and hence an accomodation coefficient of only 2×10^{-3} would yield an equilibrium system.

Hot Filament Inlet Systems

The hot filament inlet systems described below were designed for use in pyrolysis experiments at temperatures from about 900° C to the temperature at which the metallic filament collapsed. This upper temperature limit was about 1700° C for platinum and about 3000° C for tungsten.

The device shown in Figure 15 was used with gaseous samples. The parent compound was admitted from the gas-handling system described above through a monel tube (A). This tube ejected gas onto the metallic

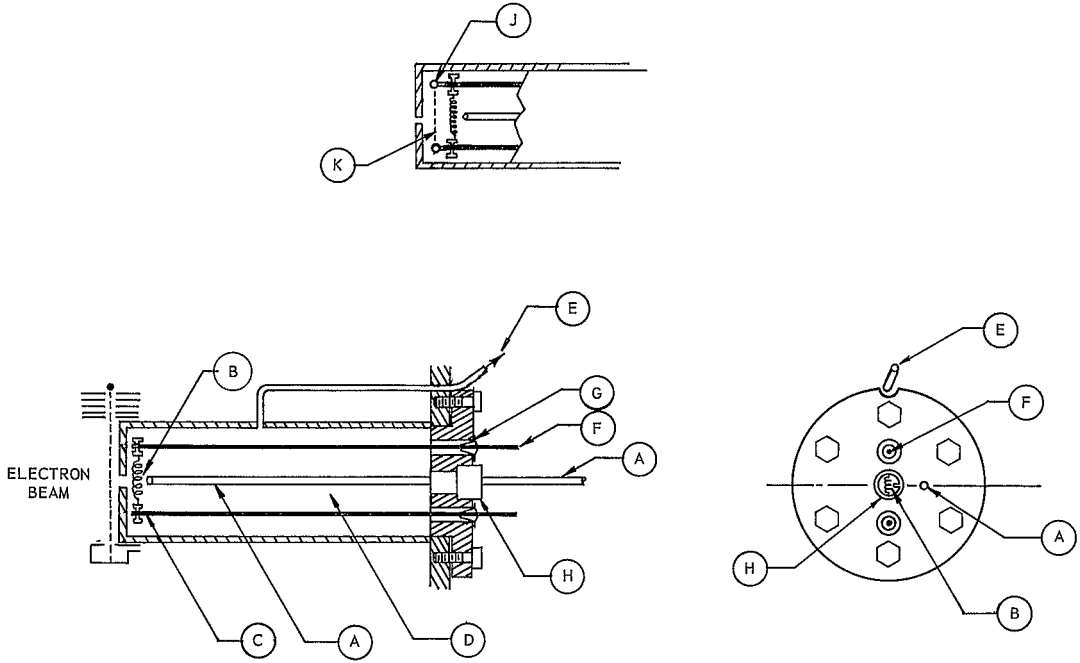

Figure 15. Hot Filament Inlet System for Gaseous Samples. (The insert shows the grid used to prevent passage of externally produced ions into the mass spectrometer.)

filament (B), which was formed into a spring-like coil. A portion of the gas then passed through a 0.032 in. leak (C) into the electron beam of the mass spectrometer. The filament was positioned approximately 1/8 in. from the electron beam to insure molecular flow.

It was found that the use of the gold foil leak described above was unnecessary since at the pressures at which the intermediate pumping volume (D) was operated the flow rate into the mass spectrometer was adequately small through the 0.032 in. orifice in the re-entrant well. This space was pumped through the line (E) by an auxiliary pumping system. Power was supplied to the filament through two brass support rods (F) which were insulated from the header by high vacuum electrical feed-throughs (G).

The temperature of the filament was measured by a Leeds and Northrup optical pyrometer, Model 8622-C. The filament was observed through a plexiglass window (H), and the instrument readings were recorded without further correction. Because of the small size of the target, the reproducibility of these measurements was only about $\pm$ 10° C. The filament current was supplied from a Sola constant voltage transformer and was regulated by a Powerstat. Fine control was provided by a 110 ohm slidewire resistor, manufactured by James G. Biddle Co., in series with the filament.

It was found that the use of a tungsten filament at high temperatures resulted in the production of a considerable number of ions in the inlet system. These ions could have been formed by surface ionization or by the acceleration of electrons between the two filament supports. In order to prevent the passage of these ions into the mass spectrometer

and the consequent large increase in the background noise in the spectrum, the retarding grid shown in the insert in Figure 15 was installed. Glass rods (J) were attached to the brass filament support rods and very fine stainless steel mesh (K), taken from a discarded ion grid, was stretched across these glass supports. This modification necessitated the movement of the filament to a position approximately 3/8 in. from the electron beam. A 6 volt positive bias was applied between this retarding grid and the filament by means of an external battery. The ion current due to ions generated outside the electron beam was thereby reduced to a level which was difficult to detect. This undesirable side effect was not observed during the use of a platinum filament.

The inlet system shown in Figure 16 was constructed for use in experiments involving parent compounds which are solids at room temperature. The filament (A) was held between the leads of two high vacuum electrical feed throughs (B) which were mounted on a small header (C). The sample tube (D) passed through the header directly under the filament.

This header was mounted on a 1 in. tube (E) and positioned so that the filament was within 1/8 in. of the leak (F) into the ion source. As in the other inlet systems, a diffusion pump separate from the mass spectrometer was used to exhaust the intermediate pumping volume (G) through the exit line (H). A window for observation of the filament was not provided in this inlet system. Settings of the Powerstat and slidewire which were required to produce certain temperatures in filaments of a particular resistance were determined in the hot filament inlet system for gaseous samples. These same settings were used to approximate these temperatures in this system.

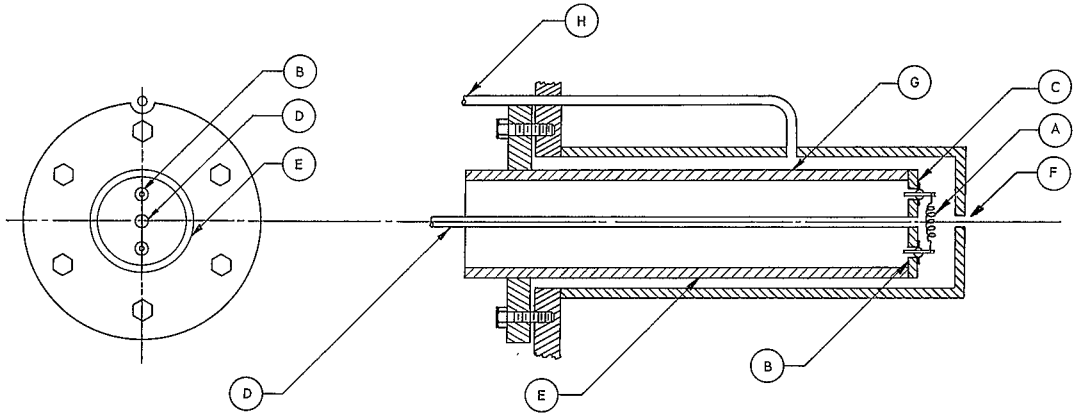

Figure 16. Hot Filament Inlet System for Solid Parent Compounds.

Cryogenic Inlet System

The broad objectives of the low temperature experiments which employ this device have been briefly outlined in Chapter I, entitled "Introduction to the Problem." Since a complete description of the apparatus will soon be published,[29] the account presented in this section includes only such detail as is necessary for an understanding of the quenching experiments of the present work.

Figure 17 shows a cross-section of the assembly as it appears when set up for studies of the quenching of gases which have been pyrolyzed on metal filaments. The highly polished outer sleeve (A) slides through an O-ring seal into an auxiliary vacuum system which permits the removal of the cryogenic inlet system for adjustments without the necessity of breaking the vacuum in the mass spectrometer. The working portion of the unit consists, in essence, of two pots, (B) and (C), which may be independently thermostated at any desired temperature down to 4.2° K. With the pots at different temperatures, the connecting tube (D), has impressed upon it a thermal gradient whose slope, $^{\circ}K/cm$, has been found to be very nearly linear. The pots are cooled by liquid refrigerants (in this work only liquid nitrogen and liquid helium were used), and fine control over the temperature of each is provided by a resistance heater wound on the center tube and controlled by two Leeds and Northrup Speedomax H AZAR recorder controllers. By such balancing of the refrigerant rate with the "bucking" heater, any temperature above the normal boiling point of the refrigerant could be maintained.

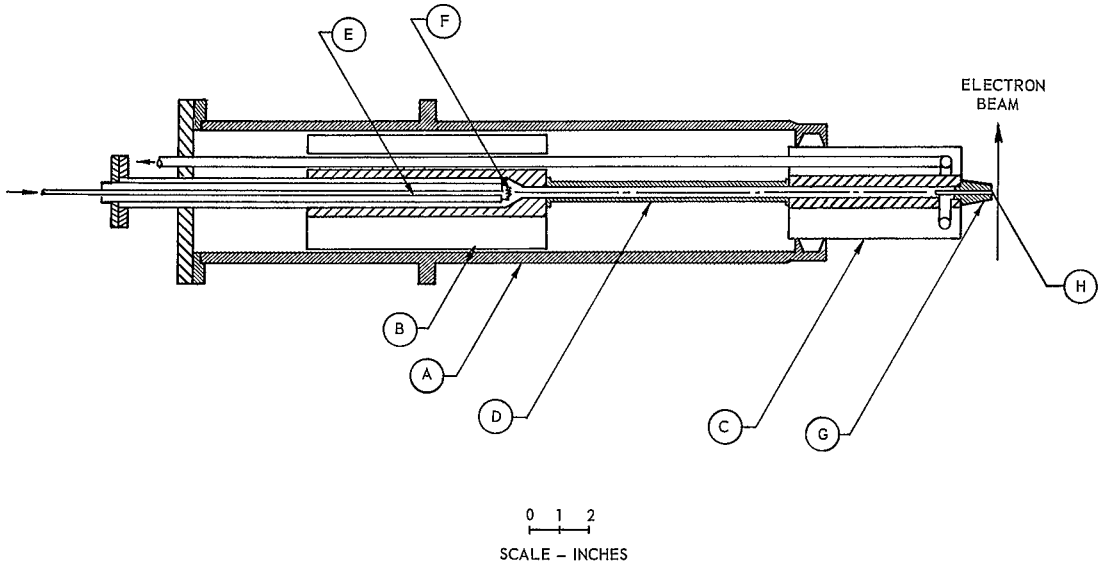

Figure 17. Schematic Diagram of Thermal Gradient Freeze-Out Assembly and Cryogenically Cooled Inlet System.

The sample gas enters at a controlled rate through the tube (E) and passes over the heated filament (F). The filament is located within 1/2 in. of the walls of pot (B) so that quenching of the pyrolysis products may be achieved very rapidly. After completion of the deposition of the sample with both pots at some low temperature, pot (B) is allowed to warm up slowly while the low temperature pot (C) is maintained at the temperature of the freezeout operation. The thermal gradient which is thus produced in the connecting tube results in a partial separation of the pyrolysis products since high vapor pressure materials will evaporate during the warmup and be condensed further down the tube. This process should yield a series of bands in the gradient tube; these bands may now be transferred down the tube and into the low temperature pot (LTP) by allowing LTP to warm while maintaining the high temperature pot (HTP) at a somewhat higher temperature.

The blade shaped snout (G) of the inlet system, which remains at essentially the same temperature as LTP, contains a delivery tube (H) (0.020 in. inside diameter) which conducts the sample gas into the mass spectrometer ionization region. This snout is positioned so that the exit of the delivery tube is directly in the ionizing electron beam; hence mass spectroscopic analysis of the vapors evolved from the low temperature bands is achieved without warmup above the temperature of LTP. This method would be expected to detect any unstable species which has a suitable vapor pressure (greater than about 10^{-2} mm Hg) below the temperature at which it decomposes or reacts.

The temperatures in HTP and LTP and along the gradient tube were determined by copper-constantan thermocouples and for use at very low

temperatures (below 77° K). constantan-chromel-p thermocouples were installed on HTP and LTP. The emf due to each of these thermocouples was measured on a Leeds and Northrup Model 8686 millivolt potentiometer.

CHAPTER III

RESULTS AND DISCUSSION

Mass Spectrometric Studies of Pyrolysis Products; Appearance Potentials and Derived Bond Energies

The production of CF_2 and CI_2 in such concentration that the free molecules could be studied in the mass spectrometer was basic to this entire study. Many parent compounds were pyrolyzed under a variety of conditions, but only a few combinations of parent and pyrolysis conditions resulted in the generation of CF_2. The highest concentration of CF_2 which was found in this work was produced by the passage of CF_3I over a heated platinum filament. None of the pyrolysis studies gave any evidence for the presence of free CI_2. The results of all of the pyrolysis experiments are briefly summarized in Table 2.

Detection and identification of the unstable species was by the method of appearance potential measurement described in the preceding Chapter. These experiments, of course, yielded a great deal of information in addition to the detection of the free CF_2 molecule. The ionization potentials of some of the parent compounds and the appearance potentials of a number of the fragment ions were measured and are given in Table 3. The most important of these results is the previously unknown ionization potential of CF_2. The mass spectra of the several parent compounds were obtained and are presented in Appendix B. Some of these spectra have not been previously reported, while others are available in standard compilations.[44] Those spectra which may be found

Table 2. Results of Pyrolysis Studies

Temperature Range	Parent Compound	Results
	- - -Tubular Furnace- - -	
100° - 500° C	CF_3I	No CF_2 Detected
	$CF_2ClCOOH$	No CF_2 Detected
	$CHClF_2$	No CF_2 Detected
Room Temp. - 300° C	C_2I_4	No CI_2 Detected; yields C_2I_2 and I_2
	CHI_3	No CI_2 Detected
	- - -Tungsten Filament- - -	
1000° - 1700° C	CF_3I	No CF_2 Detected
	CF_2CFCl	No CF_2 Detected
	Cyclo-C_4F_8	Yields C_2F_4; some evidence for CF_2
	$CHClF_2$	No CF_2 Detected
	- - -Platinum Filament- - -	
900° - 1500° C	CF_3I	CF_2 easily detected
	CF_2CFCl	Small amounts of CF_2
	Cyclo-C_4F_8	Some evidence for CF_2
	$CHClF_2$	No CF_2 Detected
	C_2I_4	No CI_2 Detected

Table 3. Appearance Potentials and Vertical Ionization Potentials

Parent Compound	Ion	Appearance Potential (ev)	Literature Value (ev)
CF_3I	CF_3I^+	10.3 ± 0.2	10.0 ± 0.3 (45)
	CF_3^+	11.1 ± 0.2	11.28 ± 0.2 (46)
	CF_2^+	17.1 ± 0.2	18.5 ± 0.6 (45)
	I^+	12.9 ± 0.2	12.9 ± 0.15 (47)
			13.6 ± 0.5 (46)
CF_2 from pyrolysis	CF_2^+	11.8 ± 0.1	13.3 ± 0.12 (48)
of CF_3I			11.7 (49)
I_2 from pyrolysis	I^+	8.8 ± 0.2	8.68 ± 0.07 (50)
of CF_3I			
cyclo-C_4F_8	CF_2^+	19.0 ± 1.0	
C_2F_4 from pyrolysis	CF_2^+	15.0 ± 1.0	15.44 ± 0.05 (47)
of cyclo-C_4F_8			
$CHClF_2$	$CHClF_2^+$	12.3 ± 0.1	12.69 ± 0.15 (51)
	CHF_2^+	12.8 ± 0.1	12.59 ± 0.15 (51)
CHI_3	CHI_3^+	9.45 ± 0.2	
	CHI_2^+	10.2 ± 0.1	
$CF_2ClCOOH$	CF_2^+	13.4 ± 0.1	

in the literature have, in almost every case, been obtained on magnetic deflection instruments and, since such spectra are not normally identical with those obtained on a time-of-flight machine, the complete low-resolution spectra which resulted from this study are reported. In addition, the mass spectra of several of these compounds were recorded at a series of temperatures and the relative intensities of their major peaks are given as a function of temperature in Appendix C.

The results of these studies are discussed in greater detail in the following pages under the headings of the respective parent compound.

CF_3I

This compound was first examined in the tubular furnace system at temperatures up to 500° C. No evidence was found for the existence of a measurable amount of CF_2 in this temperature range. The pyrolysis of CF_3I on an incandescent platinum filament, however, produced CF_2 in a concentration such that the free species could easily be studied in the mass spectrometer.

That the decomposition involved some surface effect was shown by the fact that a tungsten filament, operated at the same conditions, did not produce a detectable concentration of CF_2. Long use with other fluorocarbon vapors seemed to poison the platinum filament to such an extent that CF_2 could no longer be detected in the pyrolysis products of CF_3I.

$AP(CF_2^+)$ from CF_3I was found to be 17.1 $\pm$ 0.1 ev and, in fact, the CF_2^+ peak from CF_3I at room temperature could not be detected at electron energies below about 16 ev. When the CF_3I was passed over the

heated platinum filament (900° C - 1500° C), the CF_2^+ peak was readily observed below 16 ev and the measurement of the appearance potential of CF_2^+ from the pyrolysis products yielded $I_{vert}(CF_2) = 11.8 \pm 0.1$ ev. The ionization efficiency curves for $AP(CF_2^+)$ from CF_3I and $I_{vert}(CF_2)$ are given in Figure 18 and Figure 19 respectively. The break in the CF_2 curve at about 12.8 ev apparently corresponds to the formation of the CF_2^+ ion in an excited electronic state. There seems to be no doubt that this marked decrease in $AP(CF_2^+)$ was due to the presence of free CF_2 in the gaseous mixture and that the above value is actually the vertical ionization potential of CF_2. No other molecule of mass 50 could be formed from CF_3I and the residual air in the system. A peak appears at mass 51 when CF_3I is decomposed, but observation of the oscilloscope output showed that this peak could not contribute to the CF_2 peak at potentials near $I_{vert}(CF_2)$. The failure to detect CF_3 free radicals in the gaseous mixture would seem to eliminate the possibility that the CF_2 resulted from the electron impact fragmentation of CF_3.

The large increase in the relative height of the IF^+ peak during decomposition provided some evidence for the one-step dissociation of CF_3I into CF_2 and IF, but other processes may be formulated which would result in the production of IF.

The disproportionation of CF_3 to yield CF_2 and CF_4 (Equation (11)) has been rejected by Hodgins and Haines[52] as a possible reaction in a system containing CF_3 radicals generated from CF_3I because of the absence of CF_4 in the products.

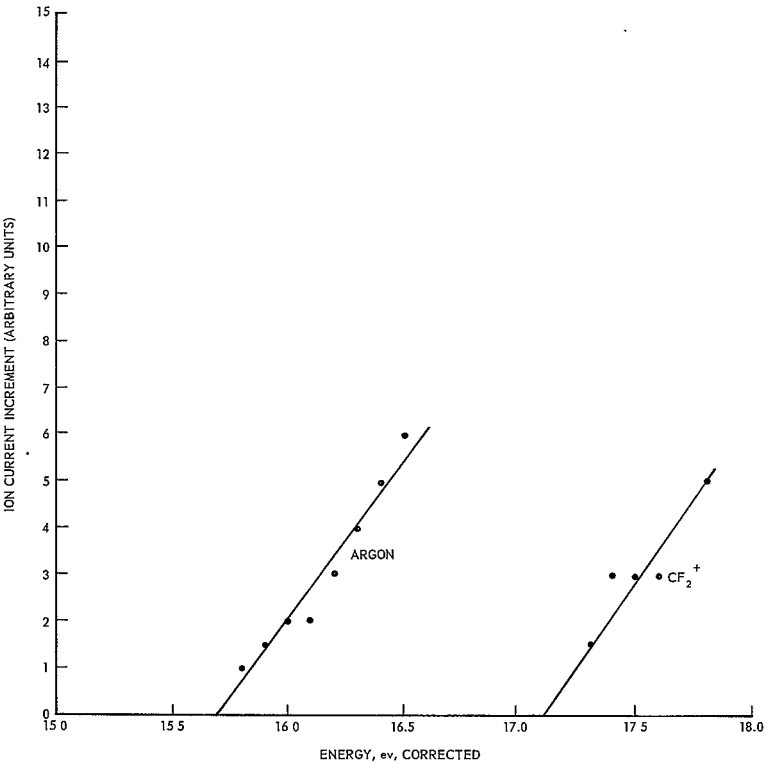

Figure 18. Ionization Efficiency Curve for AP (CF_2^+) from CF_3I.

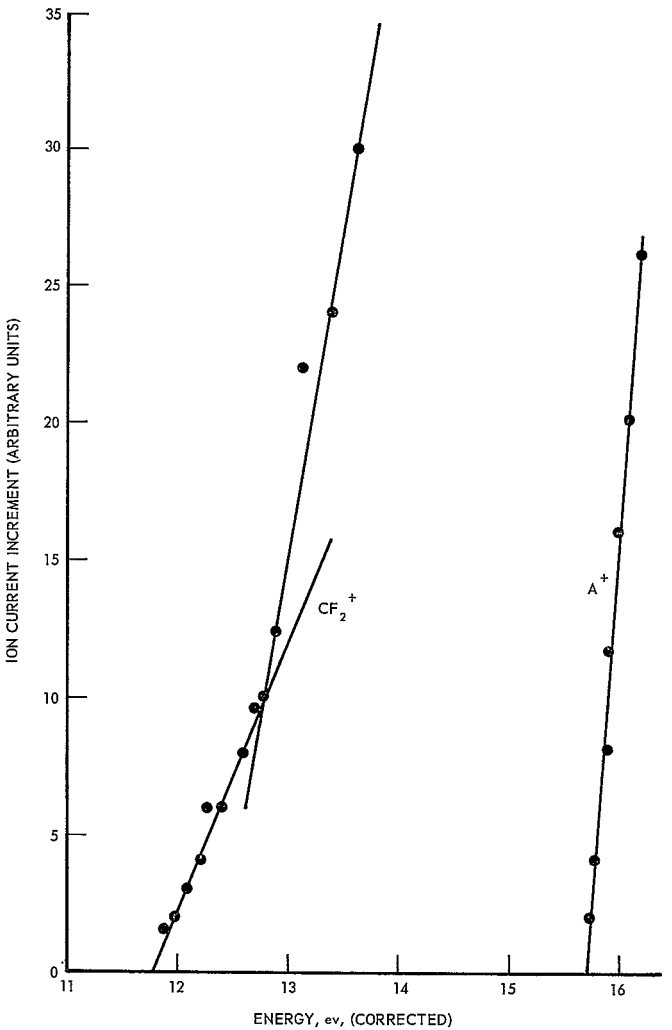

Figure 19. Ionization Efficiency Curve for I_{vert} (CF_2).

$$CF_3 + CF_3 \rightarrow CF_2 + CF_4 \qquad (11)$$

Since the mass spectrum of CF_4 is known to have no parent peak,[44] it was impossible to identify CF_4 in the hot gaseous mixture. However, the quenching experiments described later in this Chapter prove that CF_4 is present in the gas evolved from the solidified mixture after it had been quenched to liquid nitrogen temperature. Therefore, the disproportionation reaction must be considered as a possible mode of formation of CF_2.

A peak due to $C_2F_4^+$ (mass 100), which was not detected in the room temperature spectrum, was prominent in the spectrum of the pyrolysis products. Several mechanisms may be proposed to account for the formation of C_2F_4; the most obvious of these is the dimerization of CF_2. Hodgins and Haines[52] have suggested that C_2F_4 could result from the following reaction.

$$CF_3 + CF_3 \rightarrow C_2F_4 + F_2 \qquad (12)$$

In the present study this reaction must be ruled out since F_2 was not detected.

C_2F_6 and I_2 were identified as major contributors to the mass spectra of the pyrolysis products and therefore it seems highly probable that the gaseous mixture also contained significant fractions of CF_3 free radicals and I atoms. However, the CF_3 free radical was not detected by the measurement of appearance potential lowering in the pyrolysis products of CF_3I in any of these experiments and, in fact, the CF_3 peak height at low electron energies was considerably reduced when the gas

was passed over a heated platinum filament. It should be noted that $AP(CF_3^+)$ from CF_3I was found to be 11.1 ± 0.2 ev (see Figure 20) and that the ionization potential of CF_3 has been variously reported to be 8.9,[53] 9.3,[45] 9.5,[54] 10.1,[55] and 10.2[56] ev. If the high value does indeed represent $I_{vert}(CF_3)$, the appearance potential of CF_3^+ would be lowered by less than one volt upon the appearance of CF_3 free radicals in the gaseous mixture. The RPD technique utilized in this study is capable of detecting any appreciable amounts of CF_3, but of course this small lowering renders the method somewhat less sensitive.

Fisher, Homer and Lossing[49] have observed that the values in the range of 10.1-10.2 ev have been obtained by direct electron impact of CF_3 produced by thermal reactions, while the values of 8.9-9.5 were found in studies of fragmentation of CF_3 derivatives. These workers suggest that these data can be most easily reconciled by assuming that the adiabatic ionization potential of CF_3 is about 9.5 ev but that $I_{vert}(CF_3) \simeq 10.1$ ev; hence, the vertical ionization potential must include excitational energy amounting to approximately 0.6 ev.

Using their recommended value of $I(CF_3) = 9.5$ ev in Equation (10), the following estimate is obtained for the bond dissociation energy of the carbon-iodine bond.

$$\begin{aligned} D(CF_3\text{-}I) &\leq AP(CF_3^+) - I(CF_3) \\ &= 11.1 \text{ ev} - 9.5 \text{ ev} \\ &\leq 1.6 \pm 0.2 \text{ ev or } 36.9 \pm 4 \text{ kcal/mole} \end{aligned} \qquad (13)$$

The use of the lowest value of $I(CF_3)$, 8.9 ev, yields $D(CF_3\text{-}I) \leq 2.2$ ev.

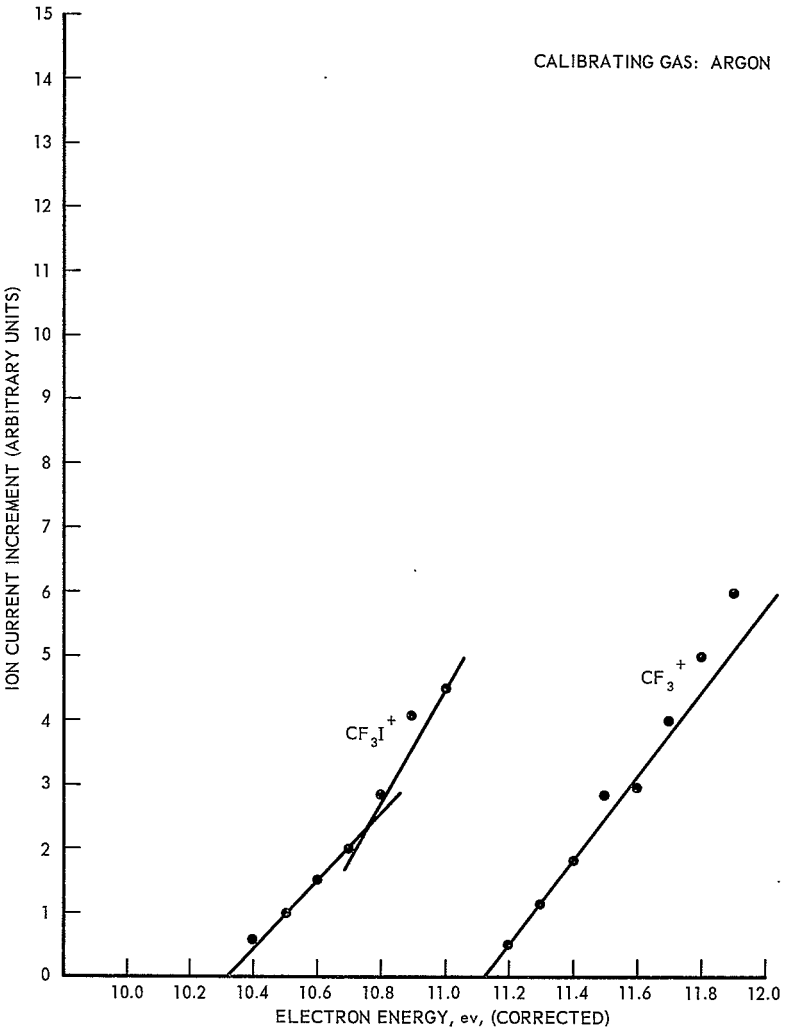

Figure 20. Ionization Efficiency Curve for AP (CF_3^+) from CF_3I and I_{vert} (CF_3I).

$AP(I^+)$ from CF_3I at room temperature was found to be 12.9 ± 0.2 ev, and the use of this value together with I(I) known from spectroscopic studies (10.6 ev)[57] in Equation (10) results in the following estimate of the carbon-iodine bond dissociation energy.

$$D(CF_3\text{-}I) \leq 12.9 - 10.6 = 2.3 \pm 0.2 \text{ ev}$$

$$= 53.0 \pm 4 \text{ kcal/mole} \qquad (14)$$

This energy is surprisingly close to the average energy of the C-I bond (57.4 kcal/mole) in the CI_4 molecule[58] and to the energy of the C-I bond in CH_3I (2.30 ev) determined by electron impact methods.[59]

A study of the negative ion spectra of CF_3I[60] has shown that the I^- ion current appears at the lowest obtainable electron energies and, hence, $D(CF_3\text{-}I)$ must be no greater than EA(I).

$$D(CF_3\text{-}I) \leq EA(I) = 3.14 \text{ ev}$$

$$= 72 \text{ kcal/mole} \qquad (15)$$

These data lend some support to the low value of $I(CF_3)$, 8.9 ev, but this support must be considered as rather flimsy since $AP(I^+)$ probably involves some excitational energy. Stevenson[61] has proposed that the dissociation of XY to give X^+ and Y can give particles of zero excitational energy only if I(X) < I(Y). By this criterion the formation of I^+ and CF_3 from CF_3I would be expected to involve some excitational energy since I(I) is at least 0.4 v greater than $I(CF_3)$.

The presence of I_2 in the pyrolysis products prevented the detection of iodine atoms since $AP(I^+)$ from I_2 is considerably lower

than I(I). Pair production again accounts for the low value of the appearance potential. The measured value of $AP(I^+)$ from I_2 (8.8 ± 0.1 ev) checks very closely with both the theoretically derived value (8.84 ev) and with that previously obtained by electron impact ($AP(I^+)$ = 8.68 ± 0.07 ev; $AP(I^-)$ = 8.62 ± 0.06).[50]

The pyrolysis of CF_3I also produces new peaks in the mass spectrum at approximately 45, 47, 51, 64, 66 and 85. Fragments of each of these masses could conceivably be produced by reaction of residual air with the dissociation products of CF_3I. Obviously, the process with which we are concerned is exceedingly complex.

Earlier studies of the decomposition of CF_3I have shown that photolysis,[62,63,64] heating[65] and reaction with sodium atoms[52] produced CF_3 radicals (identified by spectroscopic or chemical methods), but CF_2 has not been previously detected from CF_3I as a parent.

From the above observations and hypotheses several conclusions may be drawn concerning the various reactions involved in the decomposition of CF_3I on a heated platinum filament. These conclusions, and the supporting evidence for each, have been summarized in Table 4.

The importance of the determination of $I(CF_2)$ is illustrated by the work of Margrave[66] in which $I(CF_2)$ was estimated to be 11 ± 1 ev. $AP(CF_2^+)$ from C_2F_4 was found to be 15.2 ± 0.3 ev (verified in this study) and from these values $D(CF_2 = CF_2)$ was calculated by Equation (10) to be ≤ 4.2 ± 1 ev or 97 ± 23 kcal. $I_{vert}(CF_2)$, as measured in the present work, leads to the revised estimate of $D(CF_2 = CF_2) \leq$ 3.5 ± 0.2 ev or 81 ± 4 kcal. This assumes that the mode of formation of CF_2^+ does not involve pair production. Margrave[66] has pointed out

that bond energy arguments from thermochemical data[67] imply that $D(CF_2 = CF_2)$ should be about 105 kcal/mole.

The heat of formation of C_2F_4 has been shown to be -151.8 kcal/mole.[68] From this $\Delta H_f(CF_2)$ may be estimated by the use of Equation (16).

$$\Delta H_f(C_2F_4) = 2\Delta H_f(CF_2) - D(CF_2 = CF_2)$$

$$\Delta H_f(CF_2) \leq -35 \pm 2 \text{ kcal/mole} \qquad (16)$$

This result indicates that CF_2 is a rather stable molecule and is consistent with the long life time observed for CF_2.[11] A previous estimate of < - 18 kcal/mole[70] suggests considerably less stability for this molecule, but the value of ΔH_f proposed here is well above the lower limit of -45 kcal/mole determined by Thrush and Zwolenik[71] from predissociation phenomena in studies of the absorption spectra of CF_2 produced in a discharge through fluorocarbon vapors.

Fisher, Homer and Lossing[49] have very recently determined $I_{vert}(CF_2)$ to be 11.7 ev so that these two studies provide confirming results.* The free CF_2 molecules for their study were generated by the thermal decomposition of $(C_2F_5)_2N_2$ and $Hg(C_2F_5)_2$ to yield C_2F_5 radicals and the further dissociation of this radical (above 950° C) to give CF_3 and CF_2.

---

* The author expresses his appreciation to Prof. Lossing for furnishing a preprint of this paper. Prof. Lossing also made known to the author the unpublished value of $I_{vert}(CF_2)$ = 11.86 recently determined by R. F. Pottie.

Table 4. Proposed Reactions in the Decomposition of CF_3I on Platinum Filament

Proposed Reaction	Evidence From: Present Work	Evidence From: Literature on Similar Systems
$CF_3I \rightarrow CF_2 + IF$ (most likely occurs on platinum surface)	CF_2 detected by AP method. IF peak in spectrum increases very much during pyrolysis. Other reactions could give these products.	CF_2 could not be detected in photolysis of CF_3I.[9]
$CF_3I \rightarrow CF_3 + I$ (probably a surface reaction)	AP method failed to provide evidence for CF_3 or I.	Several studies have shown CF_3 to be produced in photolysis[62] and pyrolysis[65] of CF_3I.
$CF_3I + CF_3I \rightarrow C_2F_6 + I_2$	C_2F_6 and I_2 were present in quantity. Probably too much C_2F_6 to have been produced by reaction 2 followed by reaction 4.	C_2F_6 produced in several studies.[62]
$CF_3 + CF_3 \rightarrow C_2F_6$	C_2F_6 was detected.	Has been shown to proceed in a system containing CF_3.[62]
$CF_3 + CF_3 \rightarrow C_2F_4 + F_2$	No F_2 was detected. Therefore this reaction is assumed to be unimportant in this study.	Has been suggested to explain presence of C_2F_4 in such systems.[52]
$CF_3 + CF_3 \rightarrow CF_4 + CF_2$	CF_2 was detected. CF_4 was found in warmup after quenching but absence of a parent peak precluded detection in fast inlet experiments.	Proposed by several authors,[69] rejected by others because no CF_4 was found.[52]
$CF_2 + CF_2 \rightarrow C_2F_4$	C_2F_4 was detected.	Has been shown to proceed in other systems.[7]

In an earlier paper, Reed and Snedden[48] have reported $I_{vert}(CF_2)$ = 13.3 ± 0.12 ev. This work involved the pyrolysis of CF_4 on a tungsten filament and yielded a reasonable value for $I_{vert}(CF_3)$. One explanation for this rather high value for $I_{vert}(CF_2)$ is that the experiment actually determined $AP(CF_2^+)$ from CF_3 rather than $I_{vert}(CF_2)$.

The mass spectrum of CF_3I is presented in Table 8 of Appendix B.

$CF_2ClCOOH$

The usefulness of this compound as a source of CF_2 for liquid phase organic reactions has been demonstrated by Hine and Duffey.[72] These workers have shown that the chloridifluoroacetate anion ($ClCF_2COO^-$) decomposes to yield CF_2 directly without the formation of an intermediate carbanion. Hazeldine and coworkers[73] have generated CF_2 for reaction with olefins by refluxing a solution of the sodium salt for long periods of time.

$CF_2ClCOOH$ for the present study was produced by vacuum distillation from a solution of the sodium salt in concentrated H_2SO_4. The gas handling system described in Chapter II was used to admit the vapor over the liquid acid to the tubular furnace. The acid was adsorbed in this system to such an extent that its spectrum was noticeable even after the system had been pumped for several days.

Free CF_2 was not detected in the equilibrium products of the thermal decomposition of the acid at temperatures up to 500° C. The mass spectra of the pyrolysis products were recorded with the furnace at room temperature, 100° C, 200° C and 300° C and a tabulation of the relative intensities of some of the major peaks may be found in

Table 15 of Appendix C. The CF_2^+ peak was picked as the basis for these relative intensities since the height of this peak remained nearly constant with increasing temperature. Since this mass spectrum has not been previously reported, the entire spectrum at room temperature is presented in Table 9.

A study of the changes of the relative intensities with increased temperature shows that the CO_2^+ and $CClF_2^+$ peaks increase drastically while the peaks due to CF_2COOH^+, CHF_2^+ and CO_2H^+ are sharply decreased. The parent peak is absent.

There observations indicate that thermal decomposition did occur, but the mechanism of this dissociation is not obvious. The elision of CO_2 is implied by the increased CO_2^+ ion current and the decrease in the CO_2H^+ ion current, but the decreased intensity of the CHF_2^+ ion current appears to rule out the formation of CHF_2Cl since CHF_2^+ is the predominant peak in its mass spectrum.

$AP(CF_2^+)$ from $CF_2ClCOOH$ was found to be 13.4 $\pm$ 0.1 ev. The ionization efficiency curve from which this value was obtained is shown in Figure 21.

Cyclo-C_4F_8

This compound was pyrolyzed on both tungsten and platinum filaments and in each case the reaction products yielded only very meager evidence for the existence of free CF_2. The method of appearance potential measurement was again used to attempt to detect the unstable species. $AP(CF_2^+)$ from C_4F_8 was roughly found to be 19 $\pm$ 1 ev.

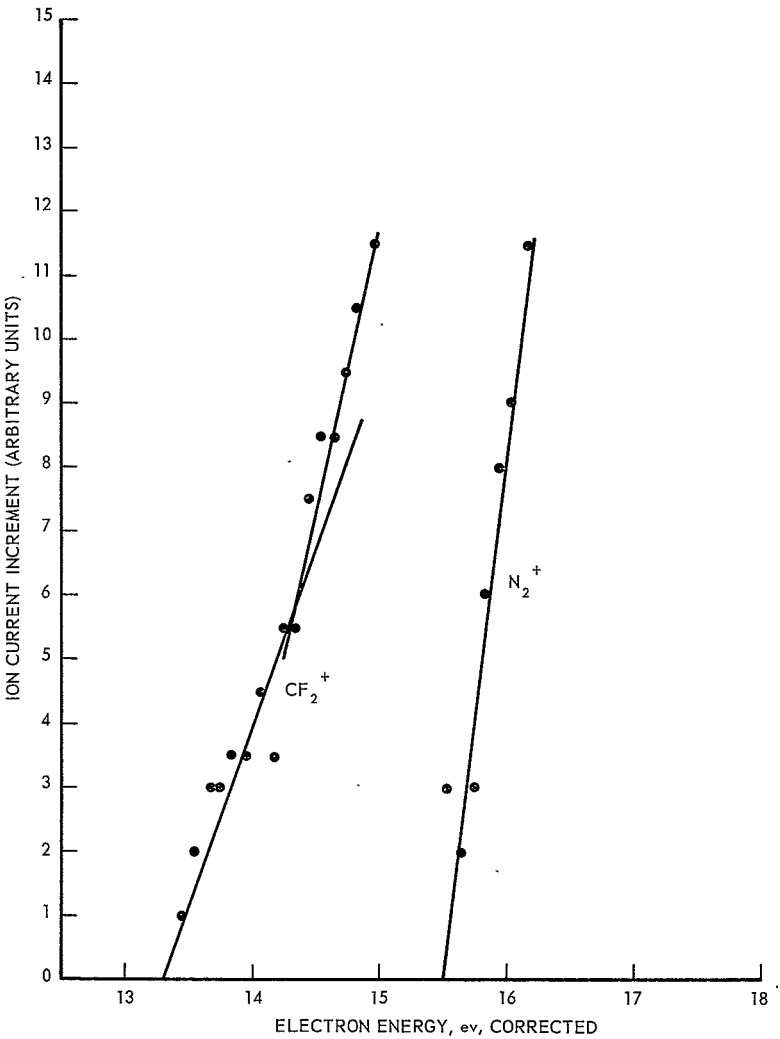

Figure 21. Ionization Efficiency Curve for AP (CF_2^+) from $CF_2ClCOOH$.

Pyrolysis on a tungsten filament resulted in a weak response to a RPD change at lower electron energies but this response was too feeble to allow an estimate of the appearance potential. The use of a platinum filament at a temperature of about 1100° C produced a lowering of the appearance potential to the neighborhood of 15 ev. The excellent agreement of this appearance potential with the value of 15.2 ± 0.3 ev reported by Margrave for AP(CF_2^+) from C_2F_4 leads to the conclusion that C_2F_4 is formed in the pyrolysis of cyclo-C_4F_8 on a platinum filament. At still higher temperatures (up to 1600° C), the CF_2^+ peak responded to a RPD change at still lower electron energies. This provided some evidence for the presence of free CF_2 but the RPD response was too weak to allow the measurement of a new appearance potential or to allow a positive identification of CF_2. The mass spectrum of cyclo-C_4F_8 is given in Table 10 of Appendix B.

$CHClF_2$

The pyrolysis of $CHClF_2$ in the tubular furnace at temperatures up to 500° C produced no indication of the presence of free CF_2 or CHF_2. The mass spectrum was recorded at a series of temperatures and the relative intensities of several peaks are tabulated in Table 16 of Appendix C. The complete mass spectrum of $CHClF_2$ is presented in Table 11 of Appendix B.

The CHF_2 peak is used as a basis for these relative intensities and it can be seen that, with the exception of the parent peak, the intensities remain almost constant. The sharp decrease in the parent peak ion current with increased temperature is consistent with the

results of previous studies of several compounds.[74] This effect has been ascribed to the increase in internal energy with temperature which puts a larger fraction of the parent molecules into a configuration from which ions can more easily be formed,[75] i.e., the ionization cross-section is increased.

$CHClF_2$ was also pyrolyzed on incandescent tungsten and platinum filaments but neither of these experiments produced free CF_2 in a concentration that could be detected by the method of appearance potential lowering.

The appearance potentials of the principal ions formed by electron impact of $CHClF_2$ have been reported by Hobrock and Kiser[51] who found that, "In the case of the CHF_2Cl, one notes that the ionization potential is slightly greater than the appearance potential for the CF_2H^+ ion. But within experimental error, these two potentials could be reversed, and very likely are. However, even from the relative abundances of the CHF_2Cl^+ and CHF_2^+ ions in the mass spectrum of chlorodifluoromethane, one would estimate that the appearance potential of CHF_2^+ would be only slightly greater than the ionization potential of this molecule." The results of the present work do not show this discrepancy but instead indicate that $AP(CHF_2^+)$ is at least 0.3 ev greater than $I_{vert}(CHF_2Cl)$. Table 5 contains the potentials obtained in each study and the ionization efficiency curves from which $I_{vert}(CHF_2Cl)$ and $AP(CHF_2^+)$ were deduced are shown in Figures 22 and 23, respectively.

Table 5. Appearance Potentials of CHF_2^+ and CHF_2Cl^+ from CHF_2Cl.

Ion	Appearance Potential	
	This Work	Hobrock and Kiser
CHF_2^+	12.8 ± 0.1	12.59 ± 0.15
CHF_2Cl^+	12.3 ± 0.1	12.69 ± 0.15

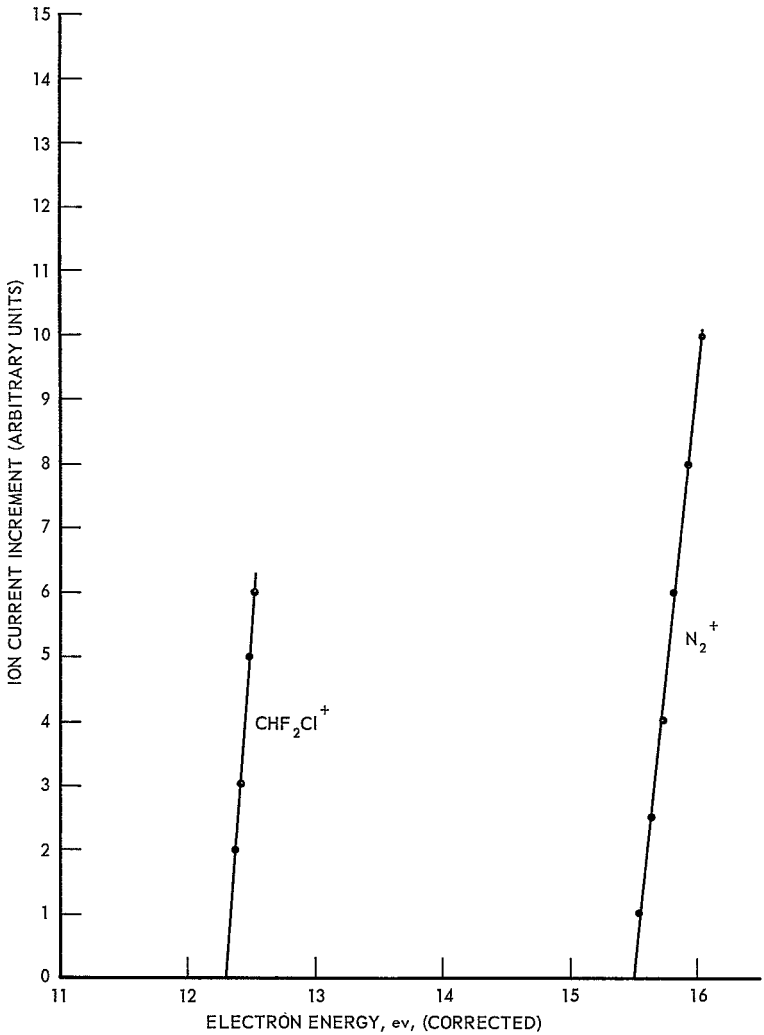

Figure 22. Ionization Efficiency Curve for IP (CHF_2Cl).

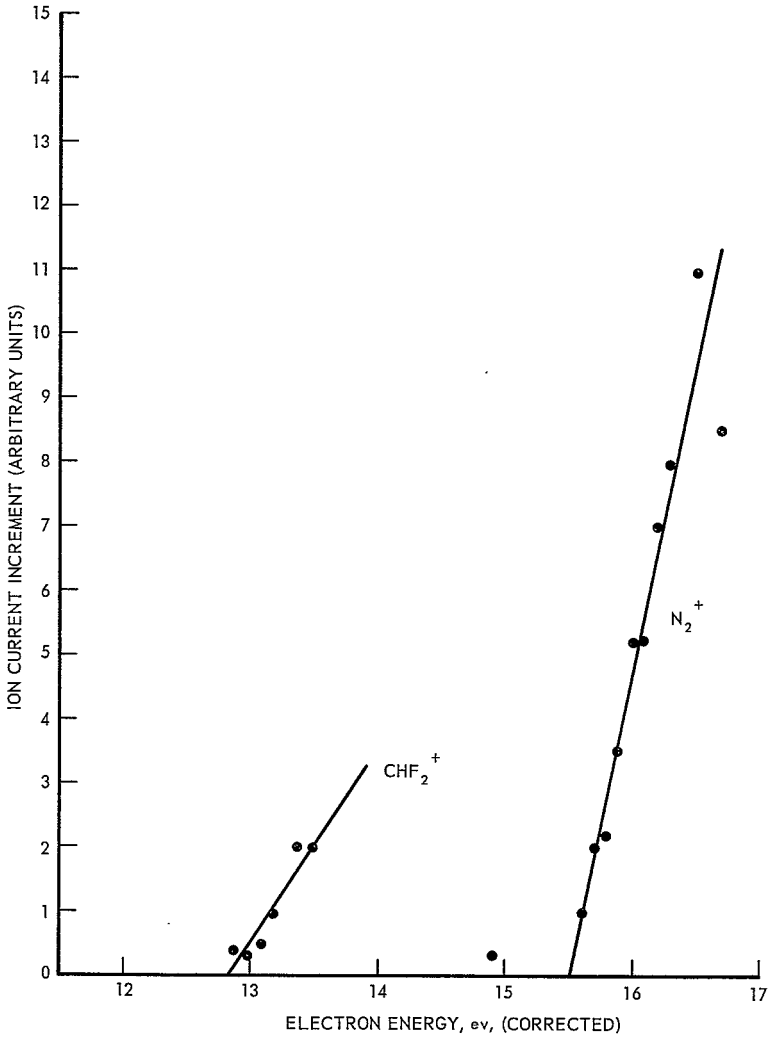

Figure 23. Ionization Efficiency Curve for AP (CHF_2^+) from CHF_2Cl.

CF_2CFCl

Free CF_2 was not detected in the effluent gases from the equilibrium pyrolysis of CF_2CFCl at tempearatures up to 500° C; likewise, no evidence was found for the production of CF_2 molecules in the passage of CF_2CFCl over an incandescent tungsten filament. However, an ion current due to CF_2^+ was observed at a significantly lowered appearance potential following the pyrolysis of CF_2CFCl on a platinum filament at temperatures above 1000° C. Unfortunately, the low intensity of this ion current made it impossible to conduct RPD studies.

The mass spectrum of CF_2CFCl is given in Table 12 of Appendix B.

C_2I_4

The pyrolysis of C_2I_4 at temperatures ranging from 100° C to 300° C was studied in the equilibrium furnace; the use of the heated inlet system was required since the solid C_2I_4 did not exert a usable vapor pressure at temperatures lower than about 85° C. No evidence was found for the presence of free CI_2 in effluent gases from the furnace but rather the data indicated that C_2I_4 decomposed into C_2I_2 and I_2. This is evidently a reversible reaction since C_2I_4 may be prepared by the reaction of C_2I_2 and I_2. This decomposition process has been noted by Heilbron and Bunbury.[76] It seems likely that this reaction occurred in the boiler as well as in the furnace since the I_2^+ ion current was more sensitive to the length of time for which the sample had been heated than to the furnace temperature. A typical mass spectrum of this material, recorded with the furnace at 125° C, is presented in Table 13 of Appendix B; the large relative intensities of I^+ and I_2^+ in

this particular spectrum imply that decomposition in the boiler had taken place, followed by vaporization of the relatively volatile iodine. The relative intensities of I^+ and I_2^+ were much lower after the sample had been heated for about 30 minutes.

The method of appearance potential measurement was used in an attempt to detect CI_2 in the gaseous products resulting from the pyrolysis of C_2I_4 on an incandescent platinum filament. No evidence was found for a lowering of $AP(CI_2^+)$ after passage of the gas over the hot filament and hence it must be concluded that this procedure does not result in the production of appreciable amounts of CI_2 from C_2I_4.

CHI_3

The pyrolysis of this interesting compound was examined in the equilibrium furnace at temperatures up to 300° C. Since CHI_3 is a solid at room temperature, the heated inlet system was again employed. There were some uncertainties in the interpretation of the mass spectra obtained in these experiments due to the difficulty of resolving adjacent mass peaks at the high mass numbers of the heavy iodine compounds. The peaks due to CI_2^+ (mass 266) and CHI_2^+ (mass 267) were not separated but careful measurement of the position of this composite peak indicates that it is due primarily to CHI_2^+. This inability to resolve the CI_2^+ peak rendered impossible any attempts to study $AP(CI_2^+)$ since it is to be expected that $AP(CI_2^+)$ will be greater than $AP(CHI_2^+)$. The ionization efficiency curve of Figure 24 shows that $AP(CHI_2^+) = 10.0 \pm 0.1$ ev and is, in fact, very low; no lowering of this AP was found in the pyrolysis of CHI_3 and hence it must be

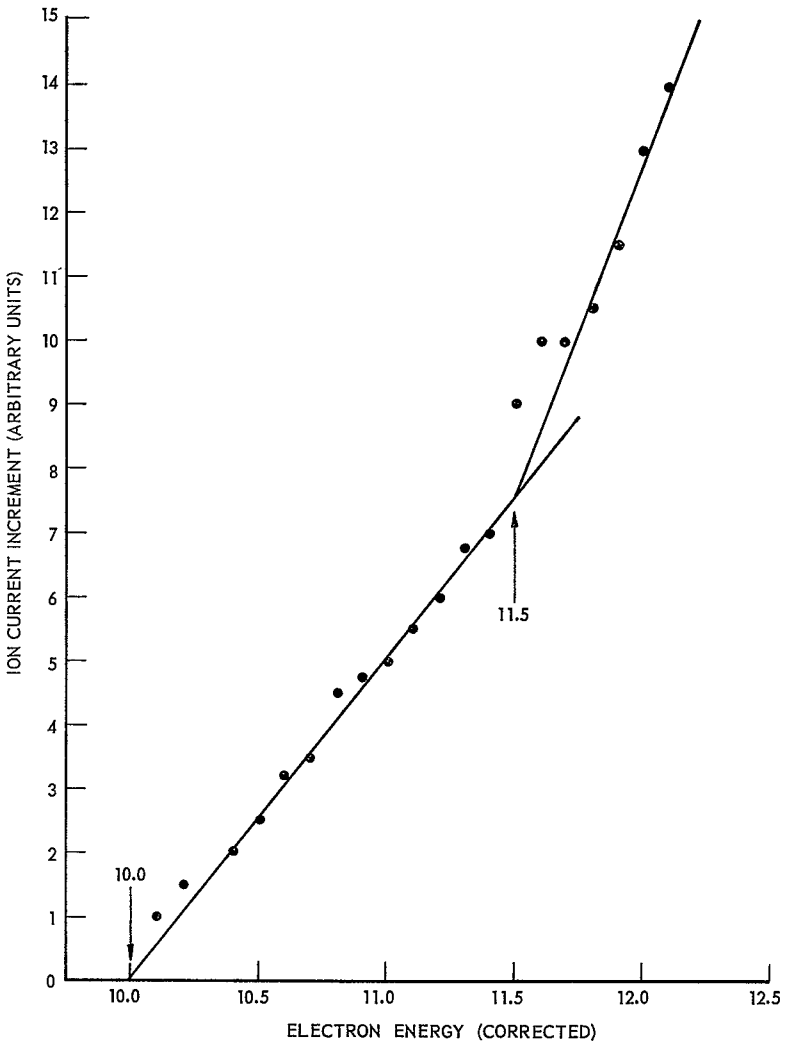

Figure 24. Ionization Efficiency Curve for AP (CHI_2^+) from CHI_3.

concluded either that no CI_2 or CHI_2 free radicals are produced or that our method is incapable of detecting these species, perhaps as a result of pair production.

$I_{vert}(CHI_3)$ was found to be 9.4 ± 0.2 ev; this indicates that ionization is from the non-bonding orbitals of the iodine atoms since this value corresponds so very closely with the ionization potentials of other iodine-containing compounds. Two such compounds are I_2 and CH_3I whose respective vertical ionization potentials are 9.41 and 9.55.[77]

The mass spectrum of this compound was recorded at 60° C, 100° C, 144° C and 300° C and the relative intensities of the major peaks at these temperatures are given in Table 17 of Appendix C. These data show the usual trend of decreased parent peak height at increased temperature but almost constant relative peak heights of the fragment ions, e.g., the cross-section for production of parent ions decreased relative to the cross-section for production of the fragment ions.

Since the mass spectrum of CHI_3 has not, to the knowledge of this author, been published, the complete low resolution mass spectrum is presented in Table 14 of Appendix B. As in the case of C_2I_4, it must be noted that this spectrum is that of CHI_3 at the temperature of the heated inlet system.

No experiments were attempted involving heated metal filaments since the lack of resolution precluded any definitive studies.

Low Temperature Quenching Experiments with CF_2

Quenching experiments on the CF_2 produced in the pyrolysis of CF_3I were conducted in the unique cryogenic inlet system described in Chapter II with liquid nitrogen or liquid helium used as the refrigerant. Since most of the experiments were conducted at liquid nitrogen temperature, this phase of the work is discussed first.

In order to duplicate as closely as possible the conditions of the experiments which resulted in the production of CF_2 (as described earlier in this Chapter), the parent compound was decomposed on a platinum filament which was set to approximately 1100° C and argon was used as a carrier gas. As indicated in Figure 17, the filament was located inside the high temperature pot (HTP) and within one-half inch of the walls of this chamber. During the pyrolysis HTP, the gradient tube and LTP were maintained at liquid nitrogen temperature so that the condensation of the hot gases was affected very close to the filament. The cracking and subsequent quenching were conducted for periods of from one-half to one hour. That this yielded an almost complete condensation of all the pyrolysis products was evidenced by the fact that in only one run was a faint spectrum due to one of these products observed while the low temperature pot (LTP) was still at liquid nitrogen temperature.

After the flow of parent gas was stopped and the hot filament turned off, the temperature of HTP was allowed to increase (usually only about 50°) while that of LTP was held at liquid nitrogen temperature. This resulted in a temperature drop along the gradient tube and,

hence, in some degree of separation of the pyrolysis products, as the more volatile species migrated down the tube toward lower temperatures. The entire inlet system was then allowed to warm slowly, while maintaining the temperature gradient, and the effluent gases were monitored (with no further warming) by the mass spectrometer. The spectra of the gases were recorded at various temperatures and the use of a discriminating low energy electron beam was employed to search for free CF_2 and CF_3.

In Table 6 are listed the fluorocarbon gases whose mass spectra were identified during the warmup and the temperature of the inlet system at the time at which these spectra were recorded. The major products were found to be CF_4, C_2F_4, C_2F_6, I_2 and the unchanged parent, CF_3I. The raw data from which these compounds were identified are presented in Appendix E accompanied by the mass spectra of each from reference 44.

CF_4 had not been previously identified in the pyrolysis studies because of the absence of a parent peak in its mass spectrum. The predominant peak in the CF_4 spectrum is that due to CF_3^+ (mass 69) and the observation of this mass at a temperature only slightly above that of liquid nitrogen, led to the initial hypothesis that the CF_3 free radical was being trapped and revaporized without reaction or recombination. However, rough appearance potential studies of this low temperature gas demonstrated that this spectrum resulted from electron impact fragmentation of the CF_4 molecule. The approximate appearance potentials of CF_2^+ and CF_3^+ from this work and the corresponding values

from Reed and Snedden's study of CF_4[48] are given in Table 7, where $I_{vert}(CF_2)$ and $I_{vert}(CF_3)$ are also given. Obviously, the first gas which is evolved during warmup must be characterized as CF_4 rather than CF_3.

At somewhat higher temperatures (about -160° C), C_2F_4 and C_2F_6 began to appear in the effluent gases from the cryogenic inlet system. The relative proportions of these gases varied from one run to another but each was present in every case. After the inlet system had warmed to about -150° C the spectrum of the unchanged CF_3I appeared; at approximately -140° C the parent compound had become the major contributor to the mass spectral pattern.

At various temperatures throughout these warmup experiments the ion currents due to the CF_2^+ and CF_3^+ ions were observed at electron energies intermediate between their ionization potentials and their appearance potentials from CF_4. In no case was there found any evidence for the presence of free CF_2 or CF_3. $AP(CF_3^+)$ did, in fact, drop to approximately 11 ev but this change was found to occur at very nearly the same temperature as that at which CF_3I began to appear in the spectrum of the warmup products ($AP(CF_3^+)$ from CF_3I = 11.1 ev).

In an additional series of experiments, liquid helium was used as a refrigerant in the cryogenic inlet system. The same pyrolysis techniques were employed but in these experiments the argon: CF_3I ratio was considerably larger (about 10:1). At 4.2° K the argon serves not only as a carrier gas but also as an inert matrix for the trapping of the unstable species.

Table 6. Gases Identified During Warmup (Liquid Nitrogen Quench)

Gas	Temperature Interval During Which Spectrum First Appeared		
	Run 1*	Run 2	Run 3
CF_4	-196° C	-196° C to -188° C	-190° C to -187° C
C_2F_4	not detected**	-188° C to -162° C	-170° C to -160° C
C_2F_6	-196° C to -150° C	-188° C to -162° C	-170° C to -160° C
CF_3I	-150° C to -192° C	-157° C to -148° C	-149° C to -142° C

* Did not record spectra between -196° C and -150° C.

** C_2F_4 was present in gases coming through the inlet system while it was being cooled simultaneously with conduct of pyrolysis. The condensed C_2F_4 must have vaporized and have been pumped out of the system in the interval between -196° C and -150° C

Table 7. AP of CF_2 and CF_3 from the Low Temperature Vapor.

	AP Obtained in this work (uncorrected)	AP from CF_4 (ref. 48)	I_{vert}
CF_2	23 ± 2 ev	22.33 ± 0.06 ev	11.8 ev
CF_3	16 ± 2 ev	15.4 ± 0.05 ev	10.2 ev[56]

In these experiments, deposition of the pyrolysis products was limited to 10-15 minutes since it was found that the cost of maintaining the system at 4.2° K was prohibitive. The cryogenic inlet system had been designed for use at liquid nitrogen temperature and a complete reconstruction would be required in order to run the system for the periods of time (about one hour) which were used for deposition in the experiments conducted at 77° K. The much smaller deposits (due both to dilution and to shorter runs) proved to be a handicap in the analysis of the warmup products since much less gas was evolved and pumped through the mass spectrometer.

The mass spectra which were recorded during the warmup of these deposits again showed the presence of C_2F_4, C_2F_6 and CF_4, but these experiments yielded no evidence for the presence of free CF_2 or CF_3 in the low temperature gas above the condensed phases which had been deposited at 4.2° K.

As mentioned in Chapter I, two recent publications[6,7] have discussed the spectroscopic study of CF_2 trapped in an argon matrix at liquid helium temperature. One of these studies,[7] which was published in September, 1964, showed that on warming to 40° K, the argon matrix softened sufficiently to permit diffusion and consequent dimerization of the trapped CF_2. After the warmed products were again cooled to 4.2° K, the spectrum of CF_2 was completely gone but that of C_2F_4 was much more intense. A personal communication from one of the authors of this latter study included this further amplification: "These studies have shown, for example, that even though CF_2 is readily formed from difluorodiazirine at 4° K in both argon and nitrogen matrices

(Inert:CF_2N_2 = 200) and can be maintained in the matrix without C_2F_4 formation for hours, at a temperature of 14° K, C_2F_4 formation is complete."* The fact that this reaction goes to completion at, or below, 14° K, indicates that the activation energy for the combination of two CF_2 molecules is extremely small and, hence, that it is highly unlikely that relatively pure samples of condensed phase CF_2 can be prepared, even at the lowest obtainable temperatures. In any event, in the present experiments, if we assume that the CF_2 survived the quench, it must have been chemically lost at temperatures well below that at which the species had enough energy to exert a vapor pressure of 10^{-2} mm Hg. The loss mechanism of the active species is examined analytically in Appendix A.

Mastrangelo[28] has studied the deposits formed by quenching to liquid nitrogen temperature the products of a radio frequency discharge in C_2F_6 or cyclo-C_4F_8. From chemical evidence, it was claimed that CF_2 was present in a blue deposit which bleached at about 95° K; and that CF_3 was present in a red deposit whose color persisted to approximately 107° K. These assignments were based on an analysis of the warmup products which resulted from chlorination and bromination of the low temperature deposits; no direct observation of CF_2 or CF_3 was reported. To reconcile these hypotheses with the more recent spectroscopic data and with the present mass spectral data, one must assume that the matrices formed by the parent compounds used in this study do

---

* The author is indebted to Dr. R. A. Mitsch of Minnesota Mining and Manufacturing Company, Saint Paul, Minnesota for this comment.

not soften and permit diffusion of the reactive species until a considerably higher temperature than is the case in an argon matrix (see analysis in Appendix A).

The present work, in which the pyrolysis products of CF_3I were immediately quenched to 77° K or to 4.2° K, has yielded no evidence for the presence of free CF_2 or CF_3 in the warmup gases. Since Milligan, et al.[7] have shown that CF_2 is indeed trapped in an argon matrix at liquid helium temperature and Mastrangelo[28] has presented convincing arguments for the stabilization of both CF_2 and CF_3 in a matrix of the parent, cyclo-C_4F_8, at liquid nitrogen temperature, it is very likely that CF_2 and CF_3 are present in the low temperature deposits produced in this work. One again concludes, therefore, that these species must achieve sufficient mobility in the matrices to permit reaction or recombination at temperatures which do not allow sublimation of the free species.

CHAPTER IV

CONCLUSIONS AND RECOMMENDATIONS

The work described in the preceding Chapters had led to the following conclusions:

1) Free CF_2 is produced in the pyrolysis of CF_3I on an incandescent platinum filament. Some evidence was found for the production of CF_2 in similar pyrolyses of cyclo-C_4F_8 and CF_2CFCl; no CF_2 was detected in the pyrolysis of $CHClF_2$.

2) CI_2 was not detected in the thermal decomposition of CHI_3 or C_2I_4.

3) The vertical ionization potential of CF_2 was found to be 11.8 $\pm$ 0.1 ev; several other vertical ionization potentials and appearance potentials were determined and are listed in Table 3 in Chapter III.

4) The method of appearance potential lowering failed to detect CF_3 in the pyrolysis of CF_3I although $AP(CF_3^+)$ from CF_3I is almost one volt more than the most probable value of $I_{vert}(CF_3)$.

5) The effluent gases from the pyrolysis of CF_3I on a platinum filament were rapidly quenched to 77° K or to 4.2° K and the gases evolved from these deposits were monitored during warmup. No CF_2 was detected in these gases and, hence, it is concluded that this unstable compound reacts or recombines in the solid deposits rather than subliming as the free species.

6) CF_4, C_2F_4, C_2F_6 and I_2 were identified in both the pyrolysis

products of CF_3I and in the gases evolved during warmup of the quenched pyrolysis products.

7) The mass spectra of CF_3I, cyclo-C_4F_8, CF_2HCl, CF_2CFCl, $CF_2ClCOOH$, CHI_3 and C_2I_4 have been obtained on the Bendix T-O-F mass spectrometer and are presented in Appendix B. These spectra do not have the precision of data obtained with high quality magnetic deflection machines.

As is always the case in research, several extensions of the present work may be proposed.

The recently synthesized compound, difluorodiazirine, CF_2N_2, may prove to be a much more suitable parent compound for the generation of CF_2 for cryogenic reactivity experiments. This parent would result in a much "cleaner" system and its pyrolysis could be conducted at a much lower temperature. The synthesis of CF_2N_2 is now classified but when a sample of this material is available it is recommended that the quenching experiments (particularly those conducted at 4.2° K) be repeated with this parent compound.

The low temperature reactivity of CF_2 toward a variety of chemicals could also be studied in the cryogenic inlet system. A compound, for example, C_2F_4, could be deposited in the inlet system and CF_2 could be generated in close proximity to this deposit; the warmup products of this reaction would be identified by monitoring the evolved gases in the mass spectrometer. Such a process might well result in the formation of new chemical intermediates which would be stable at low temperatures. Some simple molecules with which CF_2 might be reacted are CO, H_2, F_2 and Cl_2.

The recent identification of $Si(CH_3)_2$[78] suggests the possibility of the generation and mass spectrometric study of the dihalosilenes, SiX_2. The pyrolysis of SiF_4, for instance, on an incandescent wire might prove to be a suitable reaction for the production of SiF_2 in the gas phase. Timms, Ehlert and Margrave[79] have recently described several studies of the high temperature reactivity of SiF_2 generated by the pyrolysis of SiF_4 over metallic silicon at 1150° C.

The hot filament inlet systems which were designed and constructed as a portion of this work may prove to be very useful for the study of high temperature surface reactions. Operation of these inlet systems at low pressure provides an essentially collision free path from the filament into the mass spectrometer ion source so that the gases leaving the filament should be analyzed without further change.

APPENDICES

APPENDIX A

EXAMINATION OF THE STABILITY OF CF_2 IN AN ARGON MATRIX

The stability of CF_2 in a matrix of a solid material at very low temperatures is of great interest to this work and, therefore, it seems appropriate to briefly consider the conditions necessary for stabilization. Many estimates of the maximum possible concentration of frozen free radicals are available in the literature[80] but none of these seems to take into account the temperature gradient across a thin film of condensed material; this point is discussed below. The approach to the estimation of the diffusion rate which is suggested here is also thought to be unique.

The diffusion of active species through an inert matrix is thought to be a function of T/T_m, where T_m is the melting temperature of the matrix material and, specifically, it has been found that trapped free radicals usually disappear at a temperature near $\frac{T_m}{2}$.[81] Since the active material is always present in very low concentrations, it seems plausible to develop an active molecule collision rate theory by analogy to the kinetic theory of gases. The number of collisions per unit volume per second in a gas is given by

$$\pi \sigma^2 \, v \, n^2 \sqrt{2} \qquad (1)$$

where σ is the molecular collision diameter, v is the average speed and n is the number of molecules per unit volume. If we now think of our

active material as a "slow moving" gas whose "speed" is temperature dependent, we may use a similar form for frozen free radicals. The average "speed" of the species of interest in its movement through the matrix will undoubtedly be very small. In a gas the speed is proportional to the square root of temperature, but, since, the average "speed" of movement of the active species in an inert matrix is dependent on both softening of the matrix and the kinetic energy of the radicals, it seems more reasonable to assume a linear dependency on temperature, i.e., we are taking the chemical activation energy to be insignificant relative to the energy required to soften the matrix. Therefore, if we represent the number of active molecules per unit volume by n_r we find that the number of collisions per unit volume per second is proportional to

$$\pi \sigma^2 T/T_m n_r^2 \sqrt{2} . \qquad (2)$$

Since the number of recombinations will be directly proportional to the number of collisions and since σ will likely be very nearly constant over small temperature ranges, we find

$$\frac{dn_r}{dt} = - c \frac{T}{T_m} n_r^2 \qquad (3)$$

where c is a constant to be determined from the available experimental data.

At constant temperature this may be integrated to give

$$n_r = \frac{c_1}{t} + c_2 . \qquad (4)$$

This result indicates that at constant temperature the concentration of the active species will decrease as an inverse function of time.

Consider next the thin layer of condensed reactive material and inert matrix shown in Figure 25.

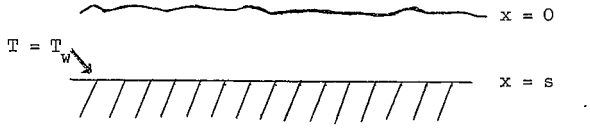

Figure 25. Schematic Showing Geometry of Reactive Film Problem.

The energy equation for this material, including the heat released by recombinations, may be written as

$$\frac{\partial T}{\partial t} = \alpha \frac{\partial^2 T}{\partial x^2} - \frac{\Delta H}{\rho c_p} \left(\frac{\partial n_r}{\partial t} \right)_x$$

or

$$\frac{\partial T}{\partial t} = \alpha \frac{\partial^2 T}{\partial x^2} + c_2 n_r^2 \, T \qquad (5)$$

The boundary conditions can be simplified, and the solution of the boundary condition equation made possible by the following substitution.

$$\bar{T} \equiv T - T_w \qquad (6)$$

Hence,

$$\frac{\partial \bar{T}}{\partial t} = \alpha \frac{\partial^2 \bar{T}}{\partial x^2} + c_2 n_r^2 \, (\bar{T} + T_w) \qquad (7)$$

and at $t = 0$, $\bar{T} = 0$; (for all x)

$x = s$, $\bar{T} = 0$; (for all time)

$x = 0$, $\frac{\partial \bar{T}}{\partial x} = 0$; (i.e., $\left(\frac{\partial T}{\partial x}\right)_{x=0} = 0$ for all time).

The final boundary condition arises since there can be no heat transfer from the outer surface of the film under conditions of low temperature and high vacuum. As a first approximation, let us assume that over short time intervals and small changes in temperature that the heat production due to recombinations is constant. If we assign the maximum value to n_r, it is clear that we are using the "worst possible" conditions since n_r can only decrease with time. Therefore,

$$\frac{\partial \bar{T}}{\partial t} = \alpha \frac{\partial^2 \bar{T}}{\partial x^2} + G \tag{8}$$

where G is the rate of heat production per unit volume divided by ρc_p. Equation (8) may be solved by a method outlined by Jakob.[82] First, if $G = 0$,

$$\frac{\partial \bar{T}}{\partial t} = \alpha \frac{\partial^2 \bar{T}}{\partial x^2} \tag{9}$$

Equation (9) is readily solved by the method of separation of variables to give

$$\bar{T} = e^{-c^2 \alpha t} [A \sin cx + B \cos cx] . \tag{10}$$

Secondly, if we set $\frac{\partial \bar{T}}{\partial t} = 0$, we obtain Equation (11) to solve

$$\frac{\partial^2 \bar{T}}{\partial x^2} + \frac{G}{\alpha} = 0 . \tag{11}$$

This is integrated directly to give

$$\bar{T} = -\frac{G}{2\alpha} x^2 + Dx + E \ . \qquad (12)$$

Combining these solutions yields

$$\bar{T} = E + Dx - \frac{G}{2\alpha} x^2 + e^{-c^2\alpha t} [A \sin cx + B \cos cx] \ . \qquad (13)$$

Applying the boundary and initial conditions, we find:

1) At $x = 0$, $\frac{\partial \bar{T}}{\partial t} = 0$ and hence

$$0 = D + ce^{-c^2\alpha t} [A]$$

or $A = D = 0$.

2) At $x = s$, $\bar{T} = 0$ and hence

$$0 = E - \frac{G}{2\alpha} s^2 + e^{-c^2\alpha t} [B \cos cs]$$

and therefore $E = \frac{G}{2\alpha} s^2$

and $\cos cs = 0$

which implies that $c = (n+1/2)\pi/s$.

Since n may take any integral value, the most general form of the equation is

$$\bar{T} = \frac{G}{2\alpha} (s^2 - x^2) + \sum_{n=0}^{\infty} e^{-(n+1/2)^2\pi^2\alpha t/s^2} B_n \cos (n+1/2)\frac{\pi x}{s} \qquad (14)$$

3) At $t = 0$, $\bar{T} = 0$, and hence

$$0 = \frac{G}{2\alpha} (s^2 - x^2) + \sum_{n=0}^{\infty} B_n \cos(n+1/2)\frac{\pi x}{s}$$

The B_n's, having units of ^{o}K, are coefficients of a Fourier series and are given by

$$B_n = \frac{-\int_0^s \frac{G}{2\alpha}(s^2-x^2)\cos(n+1/2)\pi x/s \, dx}{\int_0^s (\cos (n+1/2)\pi x/s)^2 \, dx} \qquad (15)$$

or,

$$B_n = \frac{2G\, s^2}{\alpha(n+1/2)^2\pi^3} \sin(n+1/2)\pi$$

The final result, then, is Equation (14) with the B_n's given by Equation (15). The solution has been verified by substituting into Equation (8) and performing the indicated operations.

In order to utilize this solution we must obtain estimates of the parameters s, α, and G.

A consideration of the amount of gas used in an experiment and the size of the area on which deposition is assumed to occur indicates that s will not exceed 0.1 cm.

The density of solid argon at 30^{o} K is 1.75 g/cc, the thermal conductivity of the solid is about 8.7 milliwatts/cm ^{o}K and the heat capacity is approximately 0.113 cal/gm ^{o}K.[83] These values lead to

$$\alpha = \frac{k}{\rho c_p} \sim 0.01 \text{ cm}^2/\text{sec}.$$

The work of Mitsch, et al.[7] allows us to approximate G for

(and from correspondence with these authors) that CF_2 may be maintained for many hours in argon at 4° K; that it completely disappears in some finite time at 14° K; and that at 40° K the CF_2 is quickly lost. From this we can reason that at some temperature in the neighborhood of $30\text{-}40^\circ$ K the half life of trapped CF_2 is one minute. The deposits studied by Mitsch, et al contained a maximum of 1 per cent CF_2N_2 which was subsequently photolyzed. The maximum concentration of CF_2 under these conditions would be about 4×10^{-4} moles/cm^3. If we assume that the heat released by recombination is released at a steady rate over the first minute, we find that

$$G = \frac{\left(2.0 \times 10^{-4} \frac{\text{moles } CF_2}{\text{cm}^3}\right)\left(1/2 \frac{\text{mole } C_2F_4}{\text{mole } CF_2}\right)\left(81{,}000 \text{ cal/mole } C_2F_4\right)}{60 \text{ sec } (\rho c_p)} \quad (16)$$

$$= 1.5^\circ \text{ K/sec.}$$

If the estimated heat release were sustained for 10 seconds, the temperature distribution at the end of this period would be

$$\bar{T} = \frac{G}{2\alpha}(s^2 - x^2) + B_o \exp[-(1/2)^2\pi^2\alpha(10)/s^2] \cos (1/2)\pi x/s$$

$$+ B_1 \exp[-(3/2)^2\pi^2\alpha(10)/s^2] \cos (3/2)\pi x/s + \ldots . \quad (17)$$

and, since

$$B_o = 0.39^\circ \text{ K},$$

we obtain

$$\bar{T} = \frac{1.5^{\circ}\ \text{K/sec}}{2(0.01\ \text{cm}^2/\text{sec})}\ (0.1^2-x^2)\ \text{cm}^2$$

$$+ 0.39^{\circ}\ \text{K}\ \exp[-(1/2)^2\pi^2(0.01)(10)/0.1^2]\ \cos\ (1/2)\pi x/0.1$$

$$+ \ldots.$$

or

$$\bar{T} = 75\ (0.1^2-x^2) - 0.39\ e^{-24.6}\ \cos\ \frac{\pi x}{0.1} + \ldots.$$

and finally,

$$\bar{T} \cong 75\ (0.1^2-x^2)\ .$$

Obviously, a steady state is very quickly obtained since the time-dependent terms of this expression become insignificant at much less than 10 seconds. The maximum temperature differential ($\bar{T} = T_o - T_w$) across the thin layer will be at x = 0.

$$\bar{T}_{max} = 75\ (0.1)^2$$

$$T_o - T_w = 0.75^{\circ}\ \text{K}$$

If we now wish to include the effect of temperature on the rate of heat evolution, that is, to remove the restriction that G in Equation (8) is constant, we must solve Equation (7). This may be rewritten as

$$\frac{\partial \bar{T}}{\partial t} = \alpha\ \frac{\partial^2 \bar{T}}{\partial x^2} + a^2 \bar{T} + b \qquad (18)$$

where

$$a^2 = c_2 n_r^2$$

and

$$b = c_2 n_r^2 T_w .$$

Rather than accounting for the variation of n_r with time, we can solve this equation for the initial value of n_r and, hence, obtain a "worst possible" solution. The boundary conditions are as given for Equation (7) and the method of solution is analogous to the solution of Equation (8). First, if b = 0, we have

$$\frac{\partial \bar{T}}{\partial t} = \alpha \frac{\partial^2 \bar{T}}{\partial x^2} + a^2 \bar{T} \tag{19}$$

Equation (19) is readily solved by separation of variables to give

$$\bar{T} = e^{-c^2 t} (C \cos gx + D \sin gx) . \tag{20}$$

If we set $\frac{\partial \bar{T}}{\partial t} = 0$, we have

$$\frac{\partial^2 \bar{T}}{\partial x^2} + \frac{a^2}{\alpha} \bar{T} + b/\alpha = 0 \tag{21}$$

The solution to this equation is

$$\bar{T} = A \cos \frac{a}{\sqrt{\alpha}} x + B \sin \frac{a}{\sqrt{\alpha}} x - b/a^2 . \tag{22}$$

By combining these solutions we find the following solution to Equation (18).

$$T = A \cos \frac{a}{\sqrt{\alpha}} x + B \sin \frac{a}{\sqrt{\alpha}} x - b/a^2$$

$$+ \sum_{-\infty}^{\infty} e^{-c_n^2 t} (C_n \cos gx + D_n \sin gx) .$$

Application of the boundary conditions and initial conditions prescribes the following values for the constants.

$$B = D = 0$$

$$A = \frac{b}{a^2} \left[\frac{1}{\cos \frac{a}{\sqrt{\alpha}} s} \right]$$

$$g = \frac{(n+1/2)\pi}{s}$$

$$C_n^2 = \alpha g^2 + a^2$$

$$C_n = - A \left[\frac{\sin[(as/\sqrt{\alpha}) - (n+1/2)\pi)]}{as/\sqrt{\alpha} - (n+1/2)\pi} \right.$$

$$\left. + \frac{\sin[(as/\sqrt{\alpha}) + (n+1/2)\pi)]}{as/\sqrt{\alpha} + (n+1/2)\pi} \right]$$

$$+ \frac{2b}{a^2(n+1/2)\pi} \sin (n+1/2)\pi$$

We again find that the terms in the summation are negligible after ten seconds and, using the same values of physical properties as used above, we again find that

$$\bar{T}_{max} \cong 0.8^{o} \text{ K}$$

$$T_{o} - T_{w} \cong 0.8^{o} \text{ K}$$

These small temperature gradients would not be expected to accelerate the reaction to any extent and, hence, no chain reaction would be expected at 30-40° K for 1 per cent CF_2 in argon.

If we now suppose, as an example of the application of this method, that an increase of 3° K in the matrix temperature is sufficient to promote an autocatalytic, and very soon catastrophic, reaction, we can compute the maximum concentration of CF_2 allowed by this diffusion rate theory.

For $\bar{T}_{max} = 3^{o}$ K

$$3^{o} \text{ K} = \frac{G}{2\alpha}(0.01)$$

$$G = 6.0^{o} \text{ K/sec}$$

This requires that the molar ratio of argon: CF_2 be less than 100:4, or about 4 mole per cent active material, if stabilization is to be achieved for even very short periods of time.

Other theories of the stabilization of reactive species in inert matrices predict maximum concentrations which range from 10 per cent from statistical isolation calculations down to 0.1 per cent from much more sophisticated models. The work of Mitsch, et al demonstrated that concentrations somewhat smaller than one per cent of CF_2 in argon could be achieved and, hence, the estimate of maximum concentration found here is of the right order of magnitude, at worst.

The theory proposed here, and others as well, can be verified or rejected on the basis of a carefully conducted experiment such as outlined below. CF_2 could be formed in a solid argon deposit by photolyzing CF_2N_2 in the solid matrix at any desired temperature and a relative value of the CF_2 concentration could be obtained as a function of time by recording the intensity of one of the characteristic absorption lines of the radical. Then, according to Equation (4), a plot of $\frac{1}{t}$ vs. concentration will be linear. A value of the half life of the radical species can also be obtained from these data. Any deviations from linearity in such a plot must be ascribed to a temperature rise, and consequent softening in the film and, hence, a series of such plots, obtained at various initial concentrations and at a fixed temperature will reveal the maximum allowable concentration in the matrix at that temperature and will allow us to estimate the allowable temperature drop across the film for any initial concentration of active material. Such a verification would permit us to extend this theory to the prediction of the stability of other systems.

APPENDIX B

TABULATED MASS SPECTRA

In this Appendix are presented mass spectra for the various parent compounds studied in this work; because of the inherent instability of the output of the Bendix Time-of-Flight Mass Spectrometer, these spectra must be considered as typical rather than precise. A Bendix report[85] indicates that the maximum deviation from average values of relative intensities should be of the order of three per cent, but the results obtained in this study indicate that much larger deviations may be expected when the machine is set for relatively sensitive operations; in fact, deviations of up to 20 per cent have been observed from one run to another. It was found that more consistent data were obtained when higher sample pressures and lower machine sensitivities were used but the nature of most of the work described in this thesis required the use of a relatively high sensitivity. Statistical fluctuations in the analog output could be smoothed out by the use of a larger time constant which, coupled with a much slower scan of the spectrum, should also improve the consistency of the data.

The spectra of CF_3I, $CHClF_2$, and cyclo-C_4F_8 are available in a standard reference[44] but these earlier data were obtained on magnetic deflection mass spectrometers. Since the relative intensities of mass spectra recorded on a time-of-flight mass spectrometer are often very different from those obtained on the conventional instruments, typical

spectra of these compounds are given in the following tables. Mass spectra for CHI_3, C_2I_4, $CF_2ClCOOH$ and CF_2CFCl are not found in the standard compilations of such data and these typical spectra are presented as new information.

Table 8. Mass Spectra of CF_3I

Mass	Species	Relative Intensity
12	C	1.8
19	F	1.2
31	CF	16.5
50	CF_2	12.3
69	CF_3	94.7
127	I	79.6
139	CI	1.0
146	IF	0.9
158	CFI	0.5
177	CF_2I	30.0
196	CF_3I	100.0

Electron Energy = 50 volts

Table 9. Mass Spectra of $CF_2ClCOOH$

Mass	Species	Relative Intensity
16	O	*
17	OH	*
28	CO	*
29	COH	16.1
31	CF	25.2
35	Cl	5.0
37	Cl,i	1.5
44	CO_2	*
45	COOH—	100.0
47	CCl	26.7
48	CHCl	13.6
49	CCl,i	8.1
50	CF_2;CClH,i	36.2
51	CF_2H	49.4
60	C_2FOH	5.0
63	CO_2F	4.0
64	CO_2HF	10.6
66	CFCl	20.1
67	CHFCl	10.1
68	CFCl,i	7.6

(continued)

Table 9. Mass Spectra of $CF_2ClCOOH$ (concluded)

Mass	Species	Relative Intensity
69	$CHFCl,i$	3.5
78	C_2F_2O	10.1
79	C_2F_2OH	6.1
85	CF_2Cl	32.7
86	CHF_2Cl	33.2
87	CF_2Cl,i	10.1
88	CHF_2Cl,i	9.6
92	C_2ClO_2H	4.5
94	$C_2F_2O_2;C_2ClO_2H,i$	2.0
95	$C_2F_2O_2H$	60.5
130	$CF_2ClCOOH,p$	0

Electron Energy = 50 volts

i = isotope

p = parent

*These peaks were masked by residual gases in the mass spectrometer. Some mass numbers, which could not be formed by the elements in this compound, were discarded as impurities. Since this compound was prepared in this laboratory by acidification of the sodium salt, there is a strong probability of some contamination due to reaction or decomposition of the acid.

Table 10. Mass Spectra of cyclo-C_4F_8.

Mass	Species	Relative Intensity
12	C	0.06
19	F	0.06
24	C_2	0.03
31	CF	20.0
43	C_2F	0.25
50	CF_2	7.0
62	C_2F_2	0.11
69	CF_3	18.3
74	C_3F_2	1.0
81	C_2F_3	2.5
93	C_2F	5.7
100	C_2F_4	100.0
112	C_3F_4	1.0
131	C_3F_5	82.0
150	C_3F_6	0.06
162	C_4F_6	0.03
181	C_4F_7	0.6
200	C_4F_8	0.3

Electron Energy = 50 volts.

Table 11. Mass Spectra of CHF_2Cl

Mass	Species	Relative Intensity
12	C	2.0
13	CH	3.2
19	F	1.1
20	HF	0.2
24	CHCl,d	0.3
31	CF	15.0
32	CHF	10.3
33.5	CHFCl,d	1.1
35	Cl ——	10.4
36	HCl	1.1
37	Cl,i	3.4
38	HCl,i	0.4
47	CCl	2.7
48	CHCl	0.7
49	CCl,i	1.0
50	CF_2;CHCl,i	5.6
51	CHF_2	100.0
66	CFCl	2.0
67	CHFCl	14.0

(continued)

Table 11. Mass Spectra of CHF_2Cl
(concluded)

Mass	Species	Relative Intensity
68	CFCl,i	0.7
69	CHFCl,i	4.7
85	CF_2Cl	1.7
86	CHF_2Cl,p	2.4
87	CF_2Cl,i	0.7
88	CHF_2Cl,i	0.8

Electron Energy = 60 volts

i = isotope

d = doubly - charged ion

p = parent

Table 12. Mass Spectra of CF_2CFCl

Mass	Species	Relative Intensity
12	C	1.2
19	F	0.5
31	CF	87.3
35	Cl	6.6
37	Cl,i	2.0
47	CCl	22.9
59	CCl,i	7.8
50	CF_2	13.2
66	CFCl	48.2
68	CFCl,i	11.0
81	C_2F_3	18.3
85	CF_2Cl	28.8
87	CF_2Cl,i	9.3
97	C_2F_2Cl	22.2
99	C_2F_2Cl,i	7.1
116	C_2F_3Cl	100.0
118	C_2F_3Cl,i	32.9

Electron Energy = 40 volts

i = isotope

Table 13. Mass Spectra of C_2I_4

Mass	Species	Relative Intensity
12	C	6.6
127	I	100.0
139	CI	7.1
151	C_2I	19.0
254	I_2	22.4
266	CI_2	1.1
278	C_2I_2	30.6
405	C_2I_3	11.0
532	C_2I_4	13.1

Electron Energy = 70 volts

Mass numbers corresponding to reaction products or impurities are omitted. Sample boiler was at about 110° C and furnace was 125° C. These conditions result in the production of I_2 and C_2I_2 from C_2I_4.

Table 14. Low resolution Mass Spectrum of CHI_3.

Mass	Species	Relative Intensity
12	C	3.3
13	CH	3.3
127,128	I,HI*	100
139,140	CI,CHI**	60
254	I_2	14.2
266,267	CI_2,CHI_2**	83
393,394	CI_3,CHI_3**	26

* These mass numbers were not resolved but it appears that the peak is due predominantly to the lower mass.

** These mass numbers were not resolved but it appears that the peak in each case is due prediminantly to the higher mass.

Electron Energy = 50 ev

APPENDIX C

VARIATIONS IN MASS SPECTRA WITH TEMPERATURE

The relative intensities of some of the major peaks of $CF_2ClCOOH$, CHI_3 and $CHClF_2$ are given at a series of temperatures in this Appendix. A glance at the tabulations shows that the relative intensities of several of the major peaks of $CF_2ClCOOH$ change drastically when the inlet gas is heated from room temperature to 300° C; the relative intensities of the fragment ions in the $CHClF_2$ and CHI_3 spectra, on the other hand, remain almost constant and the only noticeable change in these two mass spectra is the decrease in the relative intensity of the parent peak with increasing temperature. This latter effect has been previously noted by several workers[74] and Stevenson[75] has attributed this to an increased internal energy which results in a larger fraction of the molecules being in configurations which permit dissociation.

The large changes in the relative intensities due to the various fragments formed from $CF_2ClCOOH$ must be caused by thermal decomposition of the parent molecule prior to entering the ion source. (This has been discussed in somewhat more detail in Chapter IV.)

Table 15. Relative Intensities of Some of the Major Peaks of $CF_2ClCOOH$ at Several Temperatures.

Mass Number	Species	Relative Intensities at Room Temp.	100° C	200° C	300° C
31	CF	82	78	125	110
44	CO_2	20	30	>500**	>500**
45	CO_2H	252	260	220	123
50*	CF_2	100	100	100	100
51	CF_2H	137	122	100	44
66	CFCl	55	53	236	73
67	CHFCl	30	28	59	59
85	CF_2Cl	82	100	200	240
86	CHF_2Cl	103	100	81	70
95	CF_2COOH	200	202	163	53

* The peak due to CF_2 is used as a basis for these relative intensities since the magnitude of this peak remains more nearly constant than do the other peak heights.

** Off-scale

Electron energy = 50 ev.

Table 16. Relative Intensities of Some of the Major Peaks of CHF_2Cl at Several Temperatures.

Mass No.	Species	Relative Intensities at Room Temp.	125° C	215° C	368° C	500° C
31	CF	18.6	18.3	18.7	18.7	19.4
50	CF_2	6.0	6.2	5.8	6.4	6.0
51	CHF_2*	100	100	100	100	100
67	CHClF	15.4	16.4	15.6	15.5	16.4
86	$CHClF_2$	2.5	2.4	2.3	2.2	1.5

*The peak due to CHF_2^+ is used as a basis for these relative intensities.

Electron Energy = 60 ev.

Table 17. Relative Intensities of Some of the Major Peaks of CHI_3 at Several Temperatures.

Mass Number	Species	Relative Intensities at 60° C	100° C	144° C	300° C
127,128	I, HI*	120	127	129	137
139,140	CI, CHI*	72	75	75	78
254	I_2	17	18	17	18
266,267	CI_2, CHI_2*	100	100	100	100
393,394	CI_3, CHI_3*	31	28	27	23

* These mass numbers were not resolved (see Table 14).

Electron Energy = 50 ev.

APPENDIX D

VERIFICATION OF THE RPD TECHNIQUE

The RPD Technique discussed in Chapter II, "Apparatus and Experimental Procedures," was checked out in this apparatus and verified by determining the ionization potentials of molecular nitrogen and oxygen. The difference between these two potentials as determined in this study is given in Table 18, together with several corresponding values from the literature.

Some of the appearance potentials which are listed in Table 3 have also been determined by other workers and most of these values are in excellent agreement. Two of these appearance potentials, with the previously obtained results are listed in Table 19.

Table 18. Ionization Potentials of Oxygen and Nitrogen.

	$IP(N_2) - IP(O_2)$
Present work	3.35 ± 0.2 ev
Spectroscopic values	3.32[77,85]
	3.0[86]
Electron impact values	3.4 ± 0.05 ev[77,85]
	3.5 ± 0.2 ev[77]

Table 19. $AP(I^+)$ From I_2 and From CF_3I.

	This Work	Previous Experimental Value	Theoretical Value
$AP(I^+)$ from I_2	8.8 ± 0.1 ev	8.68 ± 0.07 ev[50]	8.84 ev[50]
$AP(I^+)$ from CF_3I	12.9 ± 0.2 ev	12.9 ± 0.15 ev[47]	----

APPENDIX E

RAW DATA FROM QUENCHING EXPERIMENTS

In the following table, the raw data from the liquid nitrogen temperature quenching experiments are presented. These data are from Run 2. The mass spectra of CF_4, C_2F_4 and C_2F_6 from a standard reference[44] are presented for purposes of comparison.

Table 20. Raw Data from Quenching Experiments.

LTP Temp.	Relative Peak Heights						
	CF	CF_2	CF_3	C_2F_3	C_2F_4	C_2F_5	C_2F_6
-188° C	10	14.6	100				
Mass Spectrum of CF_4 from reference 44	4.4	11.1	100				
-157° C			100	79.5	36	17.3	0
Mass Spectrum of C_2F_4 from reference 44				72.2	48.5		
Mass Spectrum of C_2F_6 from reference 44			100			41.5	0

BIBLIOGRAPHY*

1. J. Hine, "Divalent Carbon," Ronald Press, New York, 1964.
2. F. O. Rice and A. L. Glasebrook, J. Am. Chem. Soc. 56, 2381 (1934).
3. G. Herzberg and J. Shoosmith, Nature 183, 1801 (1959).
4. P. Venkateswarlu, Phy. Rev. 77, 676 (1950).
5. D. E. Mann and B. A. Thrush, J. Chem. Phys. 33, 1732 (1960).
6. A. M. Bass and D. E. Mann, J. Chem. Phys. 36, 3501 (1962).
7. D. E. Milligan, D. E. Mann, Marilyn E. Jacox and R. A. Mitsch, J. Chem. Phys. 41, 1199 (1964).
8. G. Herzberg, Proc. Roy. Soc. (London) A262, 291 (1961).
9. J. P. Simons and A. J. Yarwood, Nature 192, 943 (1961).
10. J. P. Simons and A. J. Yarwood, Nature 187, 316 (1960).
11. R. K. Laird, E. B. Andrews and R. F. Barrow, Trans. Faraday Soc. 46, 803 (1950).
12. J. Hine, "Divalent Carbon," p. 40.
13. J. Hine and S. J. Ehrenson, J. Am. Chem. Soc. 80, 824 (1958).
14. W. Mahler, Inorganic Chemistry 2, 230 (1963).
15. R. A. Mitsch, Journal of Heterocyclic Chemistry 1, 59, (1964).
16. J. L. Margrave and K. Wieland, J. Chem. Phys. 21, 1552 (1953).
17. B. Atkinson and V. A. Atkinson, J. Chem. Soc., 2086 (1957).
18. B. Atkinson, Nature 163, 291 (1949).
19. T. E. Khalafawi and A. Johannin-Gilles, Compt. rend. 242, 1716 (1956).

* Abbreviations follow the form described in Chemical Abstracts, List of Periodicals, 1961. Journals beginning publication since 1961 are not abbreviated.

20. T. M. Shaw, "Formation and Trapping of Free Radicals," (ed. A. M. Bass and H. P. Broida), Academic Press, Inc., New York, N.Y., 1960, p. 47.

21. G. C. Eltenton, J. Chem. Phys. 10, 403 (1942).

22. A. M. Bass and H. P. Broida, ed., "Formation and Trapping of Free Radicals," Academic Press, Inc., New York, N.Y., 1960.

23. G. J. Minkoff, "Frozen Free Radicals," Interscience Publishers, Inc., New York, N.Y., 1960.

24. J. L. Franklin, Chem. Eng. Progr. 56 (No. 4), 63 (1960).

25. S. Aoyoma and Sakuraba, J. Chem. Soc. Japan, 62, 208 (1941).

26. A. B. Amster, J. A. Neff and A. J. Aitken, "A Survey and Evaluation of High Energy Liquid Chemical Propulsion Systems," Final Report, NASA Contract NASr-38, Stanford Research Institute, November 1, 1962.

27. H. A. McGee, Jr. and W. J. Martin, Cryogenics 2, 257 (1962).

28. S.V.R. Mastrangelo, J. Am. Chem. Soc. 84, 1122 (1962).

29. H. A. McGee, Jr., W. J. Martin and T. J. Malone, to be published.

30. M. Schmisser and H. Schroter, Angew. Chem. 72, 349 (1960).

31. M. Schmeisser, H. Schroeter, H. Schlider, J. Massonne and F. Rosskopt, Ber. 95, 1648 (1962).

32. W. C. Wiley and I. H. McLaren, Rev. Sci. Inst. 26, 1150 (1955).

33. J. D. Craggs and C. A. McDowell, Reports of Progress in Physics, 18, 374 (1955).

34. C. E. Melton and W. H. Hamill, Notre Dame Report, 1963.

35. R. E. Fox, E. M. Hickam, J. D. Grove and T. Kjeldaas, Jr., Rev. Sci. Inst. 26, 1101 (1955).

36. C. E. Melton and W. H. Hamill, J. Chem. Phys. 41, 546 (1964).

37. R. W. Kiser and E. J. Gallegos, J. Phys. Chem. 66, 947 (1962).

38. J. A. Hipple and D. P. Stevenson, Phys. Rev. 63, 121 (1943).

39. G. Herzberg, Can. J. Phys. 39, 1511 (1961).

40. R. I. Reed, "Ion Production by Electron Impact," Academic Press, Inc., New York, N.Y., 1962, p. 33.

41. C. A. McDowell, "Mass Spectrometry," (ed. C. A. McDowell), McGraw-Hill Book Company, Inc., New York, 1963, p. 506.

42. F. H. Field and J. L. Franklin, "Electron Impact Phenomena," Academic Press, Inc., New York, N.Y., 1957.

43. A.J.B. Robertson, "Mass Spectrometry," Methuen and Co., London, 1954.

44. "Mass Spectral Data," American Petroleum Institute Research Project 44, (B. J. Zwolinski, dir.), College Station, Texas, 1962.

45. V. H. Dibeler, R. M. Reese and F. L. Mohler, J. Res. Nat. Bur. Standards, 57, 113 (1956).

46. J. Marriott, Ph.D. Thesis, Univ. of Liverpool, 1954, (quoted by C. R. Patrick, "Advances in Fluorine Chemistry," Vol. 2, Butterworth and Co., London, 1961, p. 1).

47. J. B. Farmer, I.H.S. Henderson, F. P. Lossing and D.M.G. Marsden, J. Chem. Phys. 24, 348 (1956).

48. R. I. Reed and W. Snedden, Trans. Faraday Soc. 54, 301 (1957).

49. I. P. Fisher, J. B. Homer and F. P. Lossing, J. Am. Chem. Soc., in press.

50. D. C. Frost and C. A. McDowell, "Advances in Mass Spectrometry," (ed. J. Waldron), Pergamon Press, New York, N.Y., 1959, p. 427.

51. D. L. Hobrock and R. W. Kiser, J. Phys. Chem. 68, 575 (1964).

52. J. W. Hodgins and R. L. Haines, Can. J. Chem. 30, 473 (1952).

53. V. H. Dibeler, R. M. Reese, and F. L. Mohler, J. Chem. Phys. 20, 761 (1952).

54. R. Bralsford, P. V. Harris and W. C. Price, Proc. Roy. Soc. A258, 459 (1960).

55. F. P. Lossing, P. Kebarle and J. B. deSousa, "Advances in Mass Spectrometry," (ed., J. Waldron), Pergamon Press, New York, N.Y., 1959, p. 431.

56. J. B. Farmer, I.H.S. Henderson, F. P. Lossing and D.G.H. Marsden, J. Chem. Phys. 24, 348 (1956).

57. "Handbook of Chemistry and Physics," Fortieth Ed., Chemical Rubber Publishing Co., Cleveland, Ohio, 1958, p. 2546.

58. L. Pauling, "Nature of the Chemical Bond," Cornell University Press, Ithica, New York, 1960, p. 85.

59. R. I. Reed, "Ion Production by Electron Impact," Academic Press, Inc., New York, N.Y., 1962, p. 35.

60. J. D. Craggs and C. A. McDowell, Rept. Prog. Phys. 18, 374 (1955).

61. D. P. Stevenson, Dis. Faraday Soc. 10, 35 (1951).

62. J. R. Dacey, Dis. Faraday Soc. 14, 84 (1953).

63. G. Porter, Dis. Faraday Soc. 14, 133 (1953).

64. J. Banus, H. J. Emeleus and R. N. Hazeldine, J. Chem. Soc. 1950, 3041.

65. R. N. Hazeldine, J. Chem. Soc. 1950, 3037.

66. J. L. Margrave, J. Chem. Phys. 31, 1432 (1959).

67. C. R. Patrick, Tetrahedron 4, 26 (1958).

68. C. A. Neugebauer and J. L. Margrave, J. Phys. Chem. 60, 1318 (1956).

69. J. R. Dacey, Dis. Faraday Soc. 14, 135 (1953).

70. J. Reed and B. Rabinovitch, J. Phys. Chem. 61, 598 (1957).

71. B. A. Thrush and J. J. Zwolenik, Trans. Faraday Soc. 59, 582 (1963).

72. J. Hine and D. C. Duffey, J. Am. Chem. Soc. 81, 1131 (1959).

73. J. M. Birchall, G. W. Gross and R. N. Hazeldine, Proc. Chem. Soc. 1960, 81.

74. R. E. Fox and J. A. Hipple, J. Chem. Phys. 15, 208 (1947).

75. D. P. Stevenson, J. Chem. Phys. 17, 101 (1949).

76. "Dictionary of Organic Compounds," (Ed. I. Heilburn and H. M. Bunburg), Vol. 3, Oxford University Press, New York, N.Y., 1946, p. 721.

77. F. H. Field and J. L. Franklin, "Electron Impact Phenomena," Academic Press, Inc., New York, N.Y., 1957, p. 106.

78. P. S. Skell and E. J. Goldstein, J. Am. Chem. Soc. 86, 1442 (1964).

79. P. L. Timms, T. C. Ehlert and J. L. Margrave, Paper K10 presented at 148th National ACS Meeting, September, 1964, Chicago, Ill.

80. See several Chapters in Reference (22).

81. G. C. Pimentel, "Formation and Trapping of Free Radicals," (ed. A. M. Bass and H. P. Broida), Academic Press, Inc., New York, N.Y., 1960, p. 69.

82. M. Jakob, "Heat Transfer," J. Wiley, New York, N.Y., 1957.

83. "A Compedium of the Properties of Materials at Low Temperatures (Phase I)" Part I, V. J. Johnson, editor. WADD-TR-60-56, July, 1960.

84. "Accuracy of Bendix Time-of-Flight Mass Spectrometer," Bendix Form MS6A.

85. R. I. Reed, "Ion Production by Electron Impact," Academic Press, Inc., New York, N.Y., 1962, p. 71.

86. "Handbook of Chemistry and Physics," Fortieth Ed., Chemical Rubber Publishing Company, Cleveland, Ohio, 1958, p. 2548.

VITA

William Joseph Martin was born in [redacted], [redacted] on [redacted], [redacted]. He attended public schools in Somerville, Tennessee and was graduated from Fayette County High School in Somerville in 1956. He entered Georgia Institute of Technology in September 1956 and was awarded the degree of Bachelor of Chemical Engineering, Cooperative Plan, with honors in June 1961. His employer under the cooperative plan was Melpar, Inc., Falls Church, Virginia.

In June 1961 he enrolled in the Graduate Division of the Georgia Institute of Technology and completed requirements for the Master of Science in Chemical Engineering in March 1963. He was employed by the Engineering Experiment Station and received National Science Foundation Cooperative Graduate Fellowships during the academic years of 1962-63 and 1963-64.

He is a member of Phi Kappa Phi, Tau Beta Pi, the Briaerean Society and the Society of Sigma Xi.

In 1960 he was married to the former Katherine Elizabeth [redacted] of Arlington, Virginia and they have one son, William Spencer. They now live in Spartanburg, South Carolina where he is employed by the Deering-Milliken Research Corporation.